Directing egg traffic: Internal mechanosensory feedback modulates central pattern generation to coordinate ovulation in *Drosophila*

Shao-Cong Su (苏少聪)[1], Ning Zhang (张宁)[1], Ji-Yang Xing (邢霁阳)[1], Chen-Yu Li (李晨雨)[1], Dick R. Nässel[3], Cong-Fen Gao (高聪芬)[1], Shun-Fan Wu (吴顺凡)[1,2*]

Affiliations:
[1] State Key Laboratory of Agricultural and Forestry Biosecurity, College of Plant Protection, Nanjing Agricultural University, Nanjing 210095, China
[2] College of Sciences, Nanjing Agricultural University, Nanjing 210095, China
[3] Department of Zoology, Stockholm University, Stockholm, Sweden
[*]Correspondence: wusf@njau.edu.cn

D. R. Nässel Orcid ID: 0000-0002-1147-7766
D. R. Nässel e-mail: dnassel@zoologi.su.se
S. F. Wu Orcid ID: 0000-0003-0096-147X
S. F. Wu e-mail: wusf@njau.edu.cn

Significance

Mechanosensory feedback and central pattern generators (CPGs) jointly regulate rhythmic behaviors. In *Drosophila*, we found a novel pair of multidendritic mechanosensory neurons (mdn-LO) in the lateral oviducts. These neurons express the mechanosensitive channels TMC, PPK, and Piezo, with TMC being crucial for preventing egg jamming during ovulation. Mutating *tmc* leads to severe egg blockage, while PPK or Piezo mutants only reduce number of eggs laid. Mdn-LO neurons sense oviduct contractions and connect with rhythm-generating ILP7-expressing neurons in the abdominal ganglion that innervate the oviduct, thus integrating into the ovulation CPG. This work reveals how TMC-mediated mechanosensory feedback fine-tunes CPG output to ensure coordinated ovulation and successful reproduction.

Abstract

Successful reproduction requires precise coordination of muscle contractions during ovulation and the motor control has been well investigated in insects. However, the location of the central pattern generator (CPG) and the sensory feedback orchestrating this process remain poorly understood. Using *Drosophila*, we identify a novel pair of multidendritic mechanosensory neurons (mdn-LO) in the lateral oviducts that express the mechanosensitive channels TMC (transmembrane channel-like protein), PPK (pickpocket), and Piezo. We demonstrate that TMC is essential for ovulation coordination: *tmc* mutation or neuron-specific knockdown increases egg-jamming at the junction between the lateral and the common oviduct, while *ppk* or *Piezo* single mutants reduce egg-laying without causing jamming. Calcium imaging reveals that mdn-LO neurons are rhythmically activated by oviduct contractions, and chemogenetic stimulation of these neurons triggers muscle contractions. Trans-Tango and GRASP (GFP Reconstitution Across Synaptic Partners) analyses show that mdn-LO neurons form synapses with female-specific insulin-like peptide 7 (ILP7)-expressing oviduct motor neurons in the abdominal ganglion. Activating either mdn-LO or ILP7 neurons induces egg-jamming, indicating their roles within a CPG network. Whereas the ILP7 neurons are likely to coordinate oviduct muscle contractions using glutamate, we found that the co-localized ILP7 affects the rate of ovulation, but plays no role in egg jamming. Importantly, the ILP7 neurons exhibit spontaneous rhythmic calcium oscillations, which are regulated by the mechanical feedback generated by egg movement in the oviduct. This novel circuit, including the TMC-expressing mdn-LO neurons and a set of ILP7 neurons, organizes an innate behavior by coupling strategic sensory information and a CPG to ensure bilateral coordination of oviduct contractions to prevent egg jamming during oviposition.

Keywords: *Drosophila*; ovulation; mechanosensation; TMC (transmembrane channel-like protein); motoneurons; central pattern generator

Introduction

Successful reproduction in oviparous organisms relies on the precise coordination of muscle contractions during ovulation and oviposition, a process orchestrated by central pattern generators (CPGs), neural circuits that generate rhythmic motor outputs. However, the CPG mechanisms governing ovulation remain poorly understood. In insects, which are commonly oviparous, the structure of the female reproductive system and the sequence of egg-laying events are conserved. It has been found that successful reproduction requires strict and precise regulation of events to occur in coordination, including mechanisms and behaviors associated with oogenesis, follicle cell rupture, motor control of reproductive oviduct muscles to ensure ovulation, egg activation, the choice of egg-laying site, and egg deposit [1-6].

Drosophila has emerged as a genetically tractable organism well suited for analysis of reproductive behavior, and the neuronal circuitry involved in mating and post-mating events has been intensely studied [7-16]. *Drosophila* is also a favorable organism to model the motor control of ovulation and oviposition [4,8,17,18]. Although *Drosophila* virgins can ovulate, mating is commonly a trigger [18]. During copulation and transfer of sperm and seminal fluid to the *Drosophila* female also sex peptide and a few other factors are transferred and act on sensory neurons in the oviduct. These neurons signal to target neurons in the brain to induce a change in physiology and behavior of the fly, including the onset of ovulation and oviposition [11,19,20]. A mated *Drosophila* female can lay eggs up to 80 times in a day [2], each time following a stereotyped sequence. Thus, oviposition comprises ovulation, the transfer of a mature egg from the ovary to the uterus where fertilization occurs, and then the deposition of eggs after a thorough search for an optimal egg-laying site [1,4,17,21]. After each egg is laid, the female goes through a grooming program and then rests before the next egg-laying cycle [1,4].

In *Drosophila,* the mechanisms by which the mature egg is transferred from the ovary to be deposited by the ovipositor are as follows. Contractions in circular muscle in the peritoneal sheath around the ovary push the egg towards the base of the ovary and these contractions are amplified by octopamine (OA) [17,18]. The entrance of the egg into one of the lateral oviducts is enabled by the rupture of the posterior mature follicle cells surrounding the oocyte, which is triggered by the activation of matrix metalloproteinase 2 due to OA acting on the OAMB receptor [5]. Further movement through the lateral and common oviducts is caused by OA modulation of contractions in the myogenic muscle in the reproductive tract [17,18,21,22]. Thus, OA acts on two different OA receptors (OAMB and Octβ2R) to cause a series of contractions and relaxations of the muscle in the oviducts to move the egg forward. The source of OA acting on the oviduct muscle is a small set of efferent neurons in the abdominal ganglion (ABG) expressing tyramine decarboxylase (TDC), a biosynthetic enzyme for

tyramine and OA [17,18,21-23], whereas the origin of OA causing follicle cell rupture is not known. When the egg enters the common oviduct, it triggers the contraction of its muscle.

In addition to the regulatory effects of OA on oviduct contractions, a group of glutamatergic motor neurons located in the ABG, which co-express insulin-like peptide 7 (ILP7), also control the contraction of the lateral oviduct and the common oviduct [4,8,24]. In the following we call these neurons ILP7-neurons. Silencing of these ILP7-neurons causes jamming of eggs at the junction between the common and lateral oviducts [4,8,24]. These studies suggest that the signal to the oviduct muscle is mediated by glutamate and found no role for the co-localized ILP7 in muscle contractions.

The contractions of the common oviduct can be sensed by mechanosensory neurons that express pickpocket (PPK) in the common oviduct [8]. However, it remains unclear which neurons are responsible for sensing the contraction of the lateral oviducts. Further down the common oviduct, a pair of posterior uterine sensory neurons (PU neurons) sense the egg's passage into the ovipositor [1]. Another pair of motor neurons (circular muscle of the uterus; CMU neurons), possibly with feedback from PU neurons, finally activate the egg expulsion, which is followed by grooming and then a new cycle of ovulation [1].

This ovulation process relies on the highly coordinated activity of the muscles in the reproductive tract. Typically, only one egg is present in the reproductive tract at a time, and only one egg can pass through the lateral oviduct at a time, indicating a coordinated movement between the oviducts to ensure the smooth passage of the egg. As mentioned above, inhibiting female-specific ILP7 neurons leads to blockage of the egg at the junction between the lateral and common oviducts, referred to as egg jamming [4]. However, it is still unclear how the coordinated transport of the eggs into the common oviduct is controlled in *Drosophila*, but a central pattern generator (CPG) is likely involved. In insects like locusts ovulation is driven by a brain-independent CPG in the abdominal nerve cord [25-27]. However, in *Drosophila* such an ovulation CPG circuit has not been identified and it is not known how sensory feedback integrates with the CPG and motor neurons like the ILP7-expressing neurons.

Here, we address these gaps by investigating the neural circuit and mechanosensory feedback mechanisms underlying ovulation CPG function in *Drosophila*. We identify a novel pair of multidendritic mechanosensory neurons in the lateral oviducts (designated mdn-LO) that express three evolutionarily conserved mechanosensitive channels: TMC (transmembrane channel-like protein), PPK (pickpocket), and Piezo, along with the sex-determination gene doublesex (distinct from adjacent fruitless-expressing multidendritic neurons). We show that TMC is uniquely required for ovulation coordination, in contrast to PPK and Piezo. TMC

mutation or neuron-specific knockdown causes severe egg-jamming. Calcium imaging confirms that mdn-LO neurons are rhythmically activated by lateral oviduct contractions, consistent with a mechanosensory role. Using trans-Tango and GRASP analyses together with calcium imaging, we demonstrate that mdn-LO neurons form functional connections with ILP7-expressing motor neurons in the ABG. Activation of either mdn-LO or ILP7 neurons induces egg jamming. Moreover, ILP7 neurons exhibit spontaneous rhythmic calcium oscillations that are modulated by mechanosensory input from the lateral oviducts. Supporting intrinsic oscillatory properties of the ILP7 neurons, we find that they express genes associated with rhythmic calcium oscillations. Thus, the mechanosensory mdn-LO and ILP7 neurons are integral parts of the ovulation CPG circuit. Although ILP7 is produced by the ILP7-neurons, knockdown of the peptide does not affect egg jamming, but reduces the number of eggs laid, suggesting that its action is on the common oviduct rather than the lateral ones. In summary, we outline a circuit consisting of a pair of TMC-dependent mechanosensory neurons and a set of rhythm-generating ILP7 neurons that ensures smoth passage of eggs through the lateral oviducts and thereby successful ovipostion and reproduction. We furthermore describe a novel function of the evolutionarily conserved TMC channels.

Results

Loss of the transmembrane channel-like (*tmc*) gene leads to egg-jamming in *Drosophila*

The paired oviducts are the conduits between the ovaries and the uterus and are essential for ensuring optimal ovulation. Typically, only one egg can pass through the oviducts into the uterus at a time in *Drosophila*, indicating that internal sensory mechanisms coordinate this process. Regarding internal sensation within the female reproductive system, existing reports are limited to *ppk*-expressing neurons in the main oviduct that enhance *Drosophila*'s preference for acetic acid by sensing oviduct contractions [8], as well as posterior uterine (PU) sensory neurons that are activated by egg progression [1]. However, how internal sensory mechanisms within the oviduct coordinate the process of egg transport from the two lateral into the unpaired uterus (to avoid egg jamming) remains unclear.

In addition to Pickpocket (PPK), also PIEZO and Transmembrane Channel-like (TMC) proteins have been identified in the female reproductive system of *Drosophila*, though their functional roles remain unknown [8,28]. In *Drosophila*, PPK, PIEZO, and TMC are evolutionarily conserved mechanosensitive ion channels [8,28-33]. These channels have been implicated in the regulation of sexual behavior [34,35], oviposition preference [33] (Wu et al., 2019b), and feeding behavior [28,36].

Given our previous finding that *Nltmc3*, a TMC ortholog in the brown planthopper (BPH), is essential for normal ovary development and oviposition [37], we sought to investigate whether the *Drosophila* ortholog *tmc* (CG46121) plays a similar role. Using

tmc mutant flies, *tmc*^{1} [28], we conducted oviposition assays and found that egg-laying was significantly reduced compared to controls (Fig. 1A).

Since reduced egg-laying can result either from defects in ovarian development or disruptions in ovulation, we first examined whether developmental effects contributed to the phenotype. To rule out effects from mating, we initially used virgin female flies (for other experiments, unless noted otherwise, mated females were used). We assessed ovarian development in virgin *tmc*^{1} mutants by measuring ovary size and found no developmental abnormalities, in contrast to BPHs [37]. Instead, we observed significantly enlarged ovaries in *tmc*^{1} flies at both day 2 and day 7 post-eclosion compared to *w*^{1118} controls (Fig. 1B, D). The enlarged ovaries were due to the accumulation of mature eggs, suggesting a severe ovulation defect in these unmated flies (Fig. 1C, D), which was not attributable to abnormalities in egg morphology (Fig. 1—figure supplement 1).

To further confirm the role of TMC in ovulation, we reintroduced the *tmc* gene into *tmc*^{1} mutants using the *tmc-GAL4* driver line [28]. The reduced oviposition, enlarged ovaries, and accumulation of mature eggs observed in *tmc*^{1} mutants were all rescued by expressing *UAS-tmc* under the *tmc* promoter (Fig. 1A–D).

We next dissected mated *tmc* mutant females to assess ovulation. Interestingly, we occasionally observed egg-jamming at the junction where the two lateral oviducts merge into the common oviduct (Fig. 1E and Fig. 1F, respectively). The frequency of this blockage was significantly higher in *tmc* mutants than in controls. Importantly, the reintroduction of the *tmc* gene in *tmc*^{1} mutants eliminated this egg-jamming phenotype (Fig.1G). Similarly, RNAi-mediated knockdown of *tmc* in *TMC-GAL4*-expressing cells also resulted in egg-jamming (Fig. 1H–I).

Finally, we explored whether the other channels might contribute to oviposition and ovulation regulation in *Drosophila* (Figure 1—figure supplement 2). Using *ppk* mutants (*ppk*^{ESB}) and *Piezo* mutants (*Piezo*^{KO}), we observed a significant reduction in egg-laying in both strains after mating (Figure 1—figure supplement 2A). However, we did not observe increased egg-jamming in these mutants or in flies with RNAi-mediated knockdown of *ppk* or *Piezo* in TMC-GAL4-expressing cells (Figure 1—figure supplement 2B–E).

These findings indicate that TMC, specifically in *tmc-GAL4*-expressing cells, plays a key role in coordinating normal ovulation in the lateral oviducts of *Drosophila*, whereas *Piezo* and PPK do not. The disruption of TMC leads to a significantly elevated incidence of egg-jamming, whereas the other channels may affect ovulation via the common oviduct.

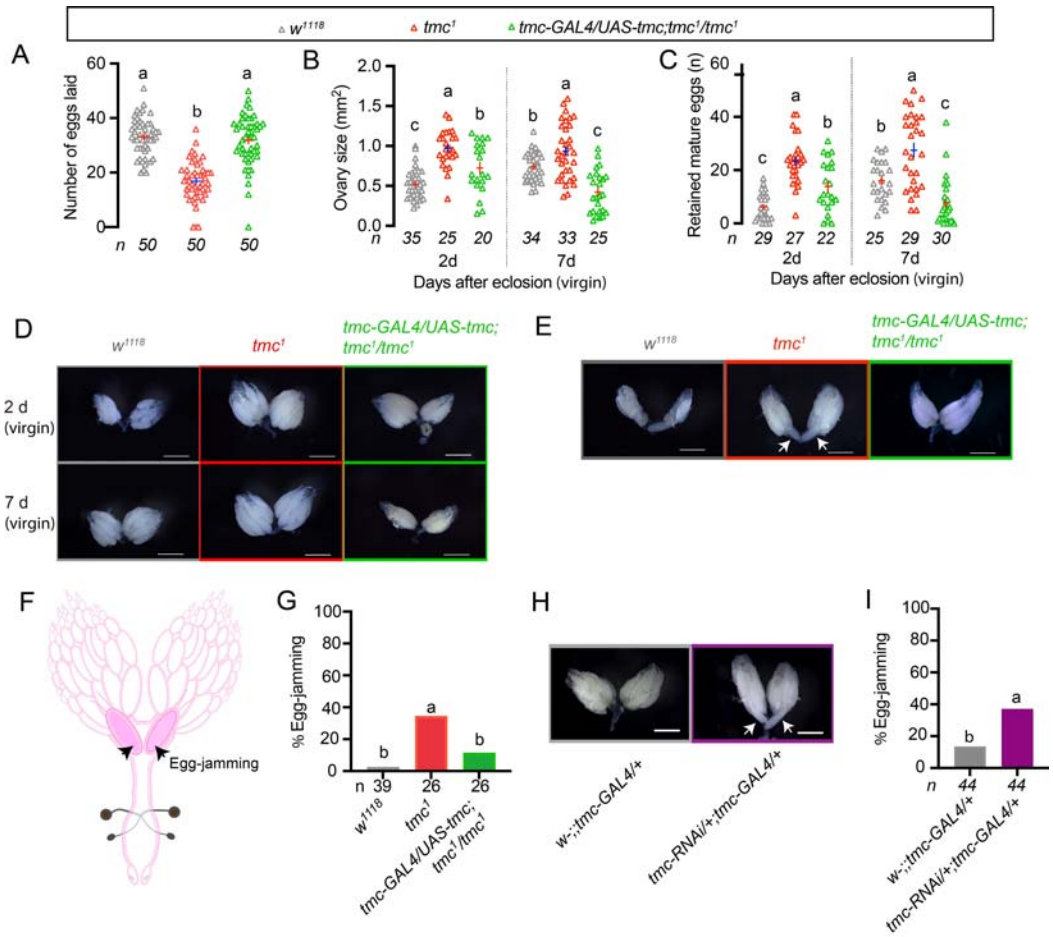

Figure 1. The *Tmc* channel is essential for ovulation and oviposition in *Drosophila*. *Tmc* mutants lay fewer eggs and display ovulation defects. All experiments, except those in Fig. 1B-D, used mated flies. Groups that share at least one letter are not statistically distinguishable ($P > 0.05$), whereas groups with completely different letters are statistically distinguishable ($P < 0.05$).

(**A**) The number of eggs laid per female of the w^{1118}, tmc^1 mutant, and *tmc-GAL4/UAS-tmc*; tmc^1 (mutant with *tmc* selectively rescued in *tmc*-GAL4-expressing cells) for 14 h at 25 °C. One-way ANOVA with Tukey's Multiple Range Test. (**B-C**) Quantification was performed on the ovary size and the number of mature eggs retained in each pair of ovaries from w^{1118}, tmc^1, and *tmc-GAL4/UAS-tmc;*tmc^1 flies. The results show that unmated tmc^1 mutant females retained more mature eggs in their ovaries, resulting in larger ovaries. This phenotype can be rescued by expressing *tmc* in neurons specifically marked by *tmc-GAL4*. Representative images of the ovaries are shown in Figure 1D. One-way ANOVA with Tukey's Multiple Range Test. (**D**) Representative images of w^{1118}, tmc^1, *tmc-GAL4/UAS-tmc*; tmc^1 ovaries on d2AAE (2 d after eclosion) and d7AEE (7 d after eclosion), from unmated flies. (**E**) Representative images of w^{1118}, tmc^1, *tmc-GAL4/UAS-tmc*; tmc^1/tmc^1 ovaries. White arrows mark the egg in the lateral oviduct. (**F**) Illustration of egg-jamming in the lateral oviduct. (**G**) The egg-jamming ratio (in %). Genotypes as in Fig 1E. Fisher's exact test. (**H**) Representative images of *w-;;tmc-GAL4/+, tmc-RNAi/+;tmc-GAL4/+* ovaries. White arrows mark the egg in the lateral oviduct. (I) The egg-jamming ratio (in %). Genotypes as in Fig. 1H. Fisher's exact test.

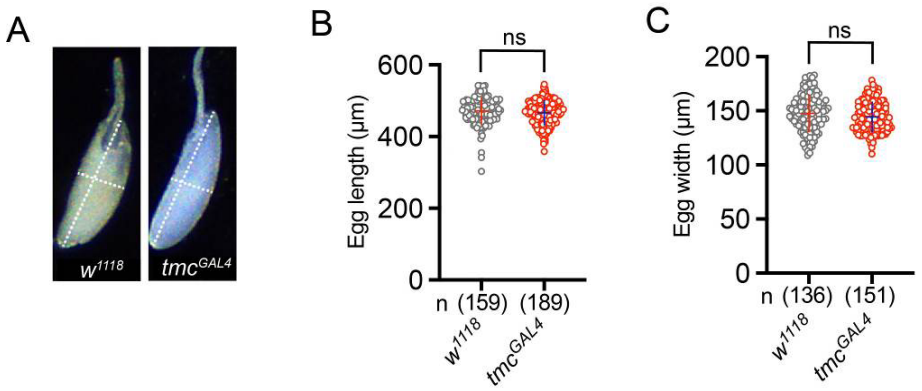

Figure 1 — figure supplement 1. The *tmc* gene does not affect egg shape.

(**A**) Representative images of eggs of w^{1118} flies and the tmc^{GAL4} mutant. (**B - C**) The egg length and width of the w^{1118} and tmc^{GAL4} mutants. Groups that share at least one letter are not statistically distinguishable ($P > 0.05$), whereas groups with completely different letters are statistically distinguishable ($P < 0.05$); Student's t-test.

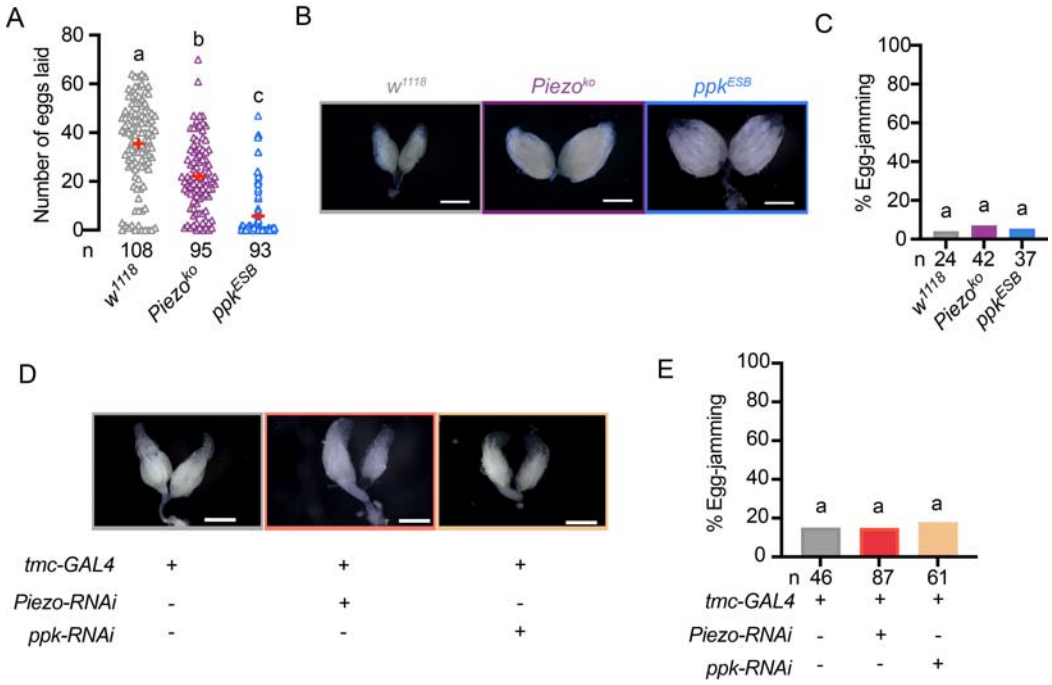

Figure 1 - figure supplement 2. Egg jamming is not affected by the manipulation of other mechanosensory channel genes.

(**A**) Number of eggs laid per female of w^{1118}, $Piezo^{ko}$, ppk^{ESB} flies for 14 h at 25 °C. One-way ANOVA with Tukey's Multiple Range Test. In this and the panels **C and E**: groups that share at least one letter are not statistically distinguishable ($P > 0.05$), whereas groups with completely different letters are statistically distinguishable ($P < 0.05$). (**B**) Representative images of w^{1118}, $Piezo^{ko}$, ppk^{ESB} ovaries. (**C**) The egg-jamming ratio. Genotypes as in **B**. Fisher's exact test.(**D**)

Representative images of *w-;;tmc-GAL4/+, ppk-RNAi/+; tmc-GAL4/+, Piezo-RNAi/+; tmc-GAL4/+* ovaries. (**E**) The egg-jamming ratio. Genotypes as in **D**. Fisher's exact test.

Tmc is localized in multi-dendritic neurons in the lateral oviduct

Whereas PPK and PIEZO have been previously localized to sensory neurons of the lateral oviducts [8], the presence of TMC in the reproductive system was hitherto not known. Thus, we set out to examine the detailed expression of this channel using a *tmc-GAL4* and by immunohistochemistry. For the latter, we generated a TMC antiserum using a previously reported method [31]. As revealed by immunocytochemical labeling and *tmc-GAL4* expression, TMC is localized in a pair of multi-dendritic neurons in the lateral oviducts that we designate **m**ulti-**d**endritic **n**eurons in the **L**ateral **O**viduct, mdn-LO (Figure 2A-B). Double-labeling experiments with TMC antibodies and *tmc-GAL4*-driven green fluorescent protein (GFP) confirmed the expression of the channel protein in these mdn-LO neurons (Figure 2A). We did not observe anti-TMC immunoreactivity in tmc^1 mutant animals, confirming the specificity of the TMC antibodies (Figure 2C). To acquire high-resolution images of the processes of the *tmc-GAL4* labeled neurons, we expressed a membrane-bound GFP (*UAS-mCD8::GFP*) under the control of *tmc-GAL4.* We found that the *tmc-GAL4* specifically identified one mdn-LO neuron in each of the two bilaterally symmetrical lateral oviducts (Figure 2D). TMC is expressed in the dendritic branches, suggesting a sensory role (Figure 2D). Each of these *tmc* neurons covers the native lateral oviduct (the one with the neuronal cell body) with their dendrites (Figure 2D). We found no *tmc*-positive sensory neuron processes in the common oviduct or the uterus (Figure 2D), where branches of PPK-positive neurons have been detected [8,38]. We also investigated the neuronal expression of two *tmc-GAL4* lines (insertions on the second and third chromosomes, respectively) and a *tmc-LexA* line in the central nervous system. Similar to previous studies [28], we found no *tmc*-positive cell bodies in the adult female ABG (Figure 2-supplemental file 1A-C), but there are many *tmc*-expressing neuronal processes projecting from peripheral tissues into the brain and ABG. This part of the ABG is a VNC region dedicated to processing female reproductive sensory input from the periphery and the origin of motor output to muscles involved in ovulation and egg-laying behavior [39] (Figure 2-supplemental file 1A-C).

We also tested whether Piezo and PPK are expressed in neurons of the lateral oviduct. Similar to previous studies [8], we observed both *Piezo-GAL4* and *PPK-GAL4* expression in multidendritic neurons in each lateral oviduct (Figure 2-supplemental file 2A and B). Next, we asked whether TMC is co-expressed with PPK or PIEZO in neurons of the lateral oviduct. Indeed, double labeling of *PPK-LexA* and *tmc-GAL4* neurons revealed that the pair of TMC-expressing mdn-LO neurons is also PPK-positive (Figure 2E). We then employed an intersectional strategy [40,41] using a combination of *tmc-GAL4*, *PPK-LexA,* and FLP recombinase to label mdn-LO neurons and observed one pair of TMC and PPK co-expressing mdn-LO neurons (Figure 2J). The axons of this pair of neurons project from the reproductive system to the ABG region of the VNC (Figure 2J-K)

Using the same approach, we examined whether Piezo and PPK, TMC and Fruitless (fru), as well as TMC and Piezo, are co-expressed in neurons of the lateral oviduct (Figure 2F–I). Taken together, our results indicate that among the two pairs of multidendritic neurons located in the lateral oviducts, one pair (mdn-LO) expresses all three channels, TMC, PPK, and Piezo, as well as Dsx (Doublesex), while the other pair expresses only PPK and fru (Figure 2L) (for Dsx, see also Rezával et al., 2012).

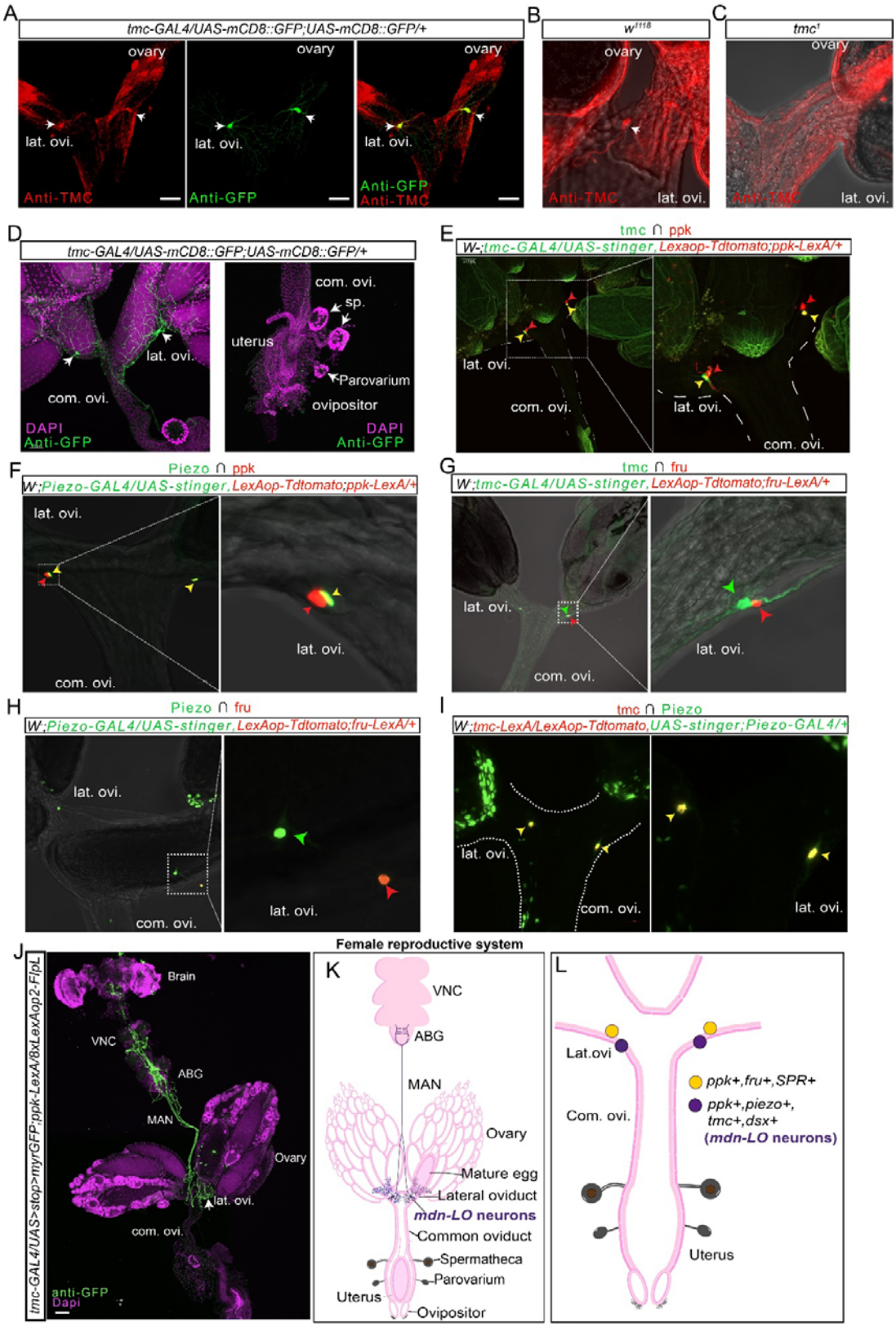

Figure 2. Expression pattern of mechanosensory channels in mdn-LO neurons

of the lateral oviducts

(A) Labeling of a lateral oviduct (lat. ovi.) with antiserum to TMC and anti-GFP staining from flies expressing the *UAS-mCD8::GFP* reporter under the control of the *tmc-GAL4*. mdn-LO neurons are indicated by arrows. **(B - C)** Labeling of the lateral oviduct (lat. ovi.) using TMC antibodies in (B) w^{1118} control and (C) tmc^{1} mutant. The arrow points to one labeled mdn-LO neuron. **(D)** TMC is specifically expressed in a pair of multi-dendritic sensory neuron cells in the lateral oviduct. Even when the egg enters the lateral oviduct, the mdn-LO neuron dendrites are still wrapped around the lateral oviduct. *tmc* is not expressed in any other part of the female reproductive system: the common oviduct (com.ovi.), spermatheca (sp.) uterus, or parovaria (female accessory glands).**(E)** Lateral oviduct neurons (mdn-LO neurons) that express both *tmc* and *ppk* are revealed by a combinatorial strategy (indicated by yellow arrows). **(F)** Lateral oviduct neurons (mdn-LO neurons) that express both *Piezo* and *ppk* are revealed by a combinatorial strategy (indicated by yellow arrows). **(G)** Lateral oviduct neurons that express *tmc* (indicated by green arrows) and *fruitless* (*fru*) (indicated by red arrows). **(H)** Lateral oviduct neurons that express *Piezo* (indicated by green arrows) and *fru* (indicated by red arrows). **(I)** Lateral oviduct neurons(mdn-LO neurons) that express both *Piezo* and *ppk* are revealed by a combinatorial strategy (indicated by yellow arrows). **(J)** Expression of *tmc* and *ppk* expressing neurons in the brain, VNC, and lateral oviducts (lat. ovi.), using the intersectional technique (*GAL4/LexA*). A distinct abdominal ganglion (ABG) region is targeted by mdn-LO neurons from the lateral oviducts. The genotype: *tmc-GAL4/UAS>stop>myrGFP;ppk-LexA/8xLexAop2-FIpL.* Common oviduct (com. ovi). median abdominal nerve (MAN). **(K)** Illustration of the morphology of the lateral oviduct *tmc-GAL4*-expressing neurons (mdn-LO) in the female reproductive system and ABG. **(L)** Summary illustration of the expression pattern of mechanosensory and other genes in lateral oviduct neurons. *Dsx*: doublesex.

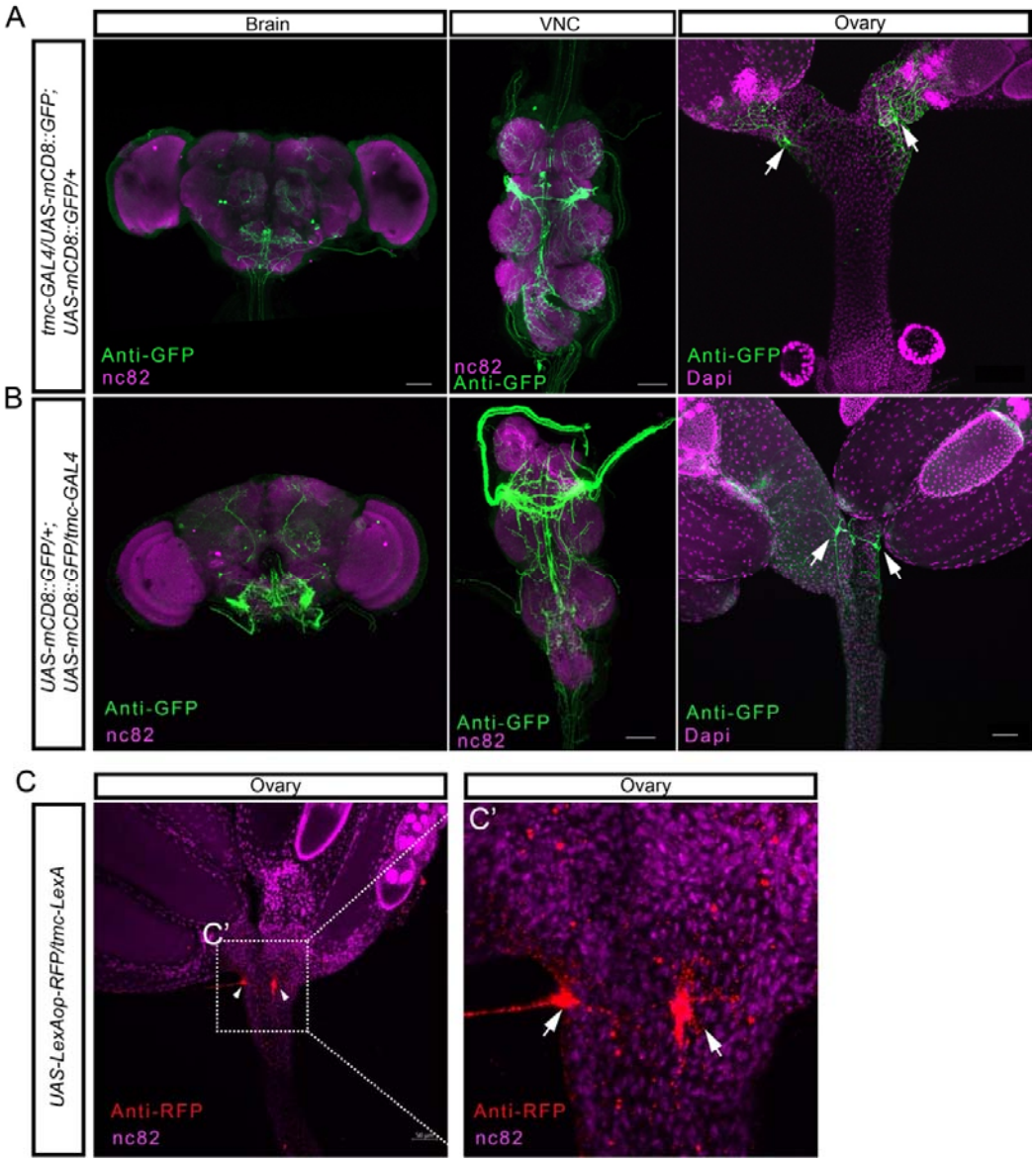

Figure 2—figure supplement 1. Expression patterns of different *tmc* drivers in the brain, ventral nerve cord, and reproductive system.

(**A-B**) Expression patterns of *tmc-GAL4* (lines with insertion on different chromosomes) expressing neurons in the brain, ventral nerve cord (VNC), and ovary. (**C**) Expression of *tmc-LexA* expressing neurons (cell bodies indicated by white arrows) in the oviduct.

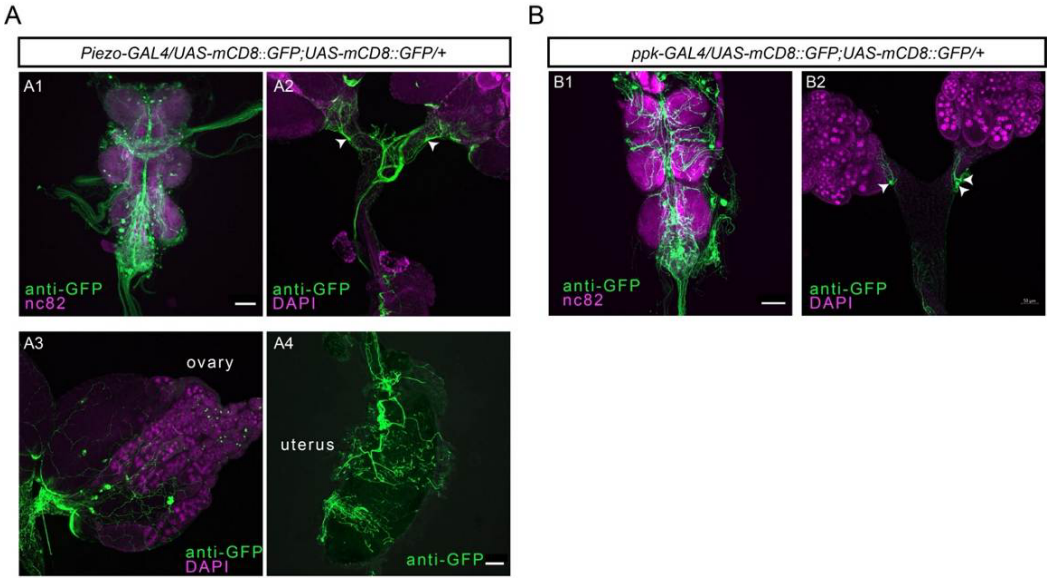

Figure 2—figure supplement 2. Expression of *Piezo* and *ppk* in CNS and reproductive tract.

(**A-B**) Expression patterns of *ppk* and *Piezo* in the female VNC (A1, B1) and reproductive system (**A2, B2**). (**A3, A4**) Expression patterns of *Piezo* in the ovary and uterus. White arrowheads mark the lateral oviduct neurons.

A pair of *Tmc*-expressing mdn-LO neurons in the lateral oviduct is essential for ovulation, and avoidance of egg-jamming

We selectively silenced the output of TMC-expressing neurons by using the *tmc-GAL4* to direct expression of the inward-rectifying potassium channel *Kir2.1* [42] and found that this manipulation causes animals to retain a similar number of eggs as the *tmc*^{1} mutants do (Figure 3A). The binding of GAL80 to the C-terminal 30 amino acids of GAL4 can prevent GAL4-mediated transcriptional activation [43] and thus inhibit the activity of GAL4 in *Drosophila* [44]. We thus silenced *tmc-GAL4* neurons with *Kir2.1* and examined the effect of *elav-GAL80* suppression of the *tmc-GAL4*-mediated transgene expression in mdn-LO neurons. Interestingly, *tmc-GAL4* > *Kir2.1* flies expressing *elav-GAL80* [45] laid almost normal numbers of eggs compared to control flies, indicating that the *tmc-GAL4* effect on oviposition is due to the mdn-LO neurons (Figure 3B). These findings show that mdn-LO neurons are necessary for normal ovulation. Furthermore, we asked whether silencing *tmc*-expressing neurons also affects ovulation coordination in *Drosophila*. However, although acute silencing of *tmc-GAL4*-expressing mdn-LO neurons with Kir2.1 reduced oviposition, it did not increase the incidence of egg jamming at the junction between the lateral and common oviducts (Figure 3C-D). We interpret this difference from *tmc* loss-of-function mutants as follows: in *tmc* mutants, mdn-LO neurons are present and active but fail to properly transduce mechanical stimuli, thus producing a defective sensory drive to the motor circuit and thereby promotes jamming. In contrast, silencing mdn-LO output removes the sensory drive altogether, yielding a state in which fewer eggs reach the

junction, leading to reduced oviposition without increased jamming.

Next, we selectively activated the output of TMC-expressing neurons thermo-genetically by using the *tmc-GAL4* to direct the expression of dTrpA1 [46]. Activation of *tmc*-GAL4 neurons via dTrpA1 (at 30°C) severely impaired oviposition (Figure 3F) and induced a significant egg-jamming rate (Figure 3G and H). To clarify which of the *tmc-GAL4* neurons are functionally required for coordinated oviposition and avoidance of egg-jamming, we suppressed the activity of GAL4 in selected tissues and cell types using the GAL80 repressor [44]. For this, we used two GAL80 lines, *elav-GAL80* [45] and vesicular glutamate transporter (*vGlut*)-*GAL80* [47]. We found that *elav-GAL80* and *vGlut-GAL80* lines both block the expression of TMC in mdn-LO neurons in the lateral oviduct (Figure 3E, Figure 3—figure supplement 1). Given that the motor neurons controlling muscle movements in *Drosophila* are glutamatergic [48], *vGlut-GAL80* serves to repress any potential GAL4 miss-expression in motor neurons.

To determine if the behavioral abnormality was due to the mdn-LO neurons, we combined the *elav-GAL80* or *vGlut-Gal80* transgene with the *tmc-GAL4* and *UAS-dTrpA1* to suppress activation of mdn-LO neurons. We found that these animals showed no difference in egg-jamming compared with control flies, while *tmc-GAL4/UAS-dTrpA1* animals showed an increased egg-jamming ratio at 30°C (Figure 3G and H).

We next used an intersectional strategy to recruit the overlapping expression of *PPK-LexA* and *tmc-GAL4* (using *tmc-GAL4/UAS>stop>myrGFP; ppk-LexA/LexAop2-FlpL*) to obtain a more precise target for our manipulations of mdn-LO neurons. However, in these flies, we observed only one of the two mdn-LO neurons (Figure 3—figure supplement 2A and figure supplement 3), possibly due to the weak cleavage efficiency of the *Flp* in the neurons. When we activated these *tmc/PPK*-coexpressing neurons using the dTrpA1 we found that these females (*tmc-GAL4/UAS>stop>dTrpA1; ppk-LexA/LexAop2-FlpL*) laid more eggs at 30°C than at 20°C (Figure 3—figure supplement 2B). In addition, we observed no ovulation deficiency or egg-jamming when we activated this single mdn-LO neuron (Figure 3—figure supplement 2C-D). These results indicate that a single mdn-LO neuron in one of the lateral oviducts is sufficient for ovulation.

To further confirm our findings, we used the optogenetic effector CsChrimson [49], which affords greater control over the dynamic range of neuronal activation than *dTrpA1* [50], and found that optogenetic stimulation of *tmc-GAL4* labeled neurons in *UAS-CsChrimsonVenus/tmc-GAL4* females abolished oviposition, dramatically different from all control females [see also [33]]. We also observed a significant egg-jamming rate in the activated *UAS-CsChrimsonVenus/tmc-GAL4* females (Figure 3I and J). Combining pan-neuronal expression of GAL80 with *UAS-CsChrimsonVenus/tmc-GAL4* significantly reduces the rate of egg-jamming seen after photoactivation (Figure 3J).

Figure 3

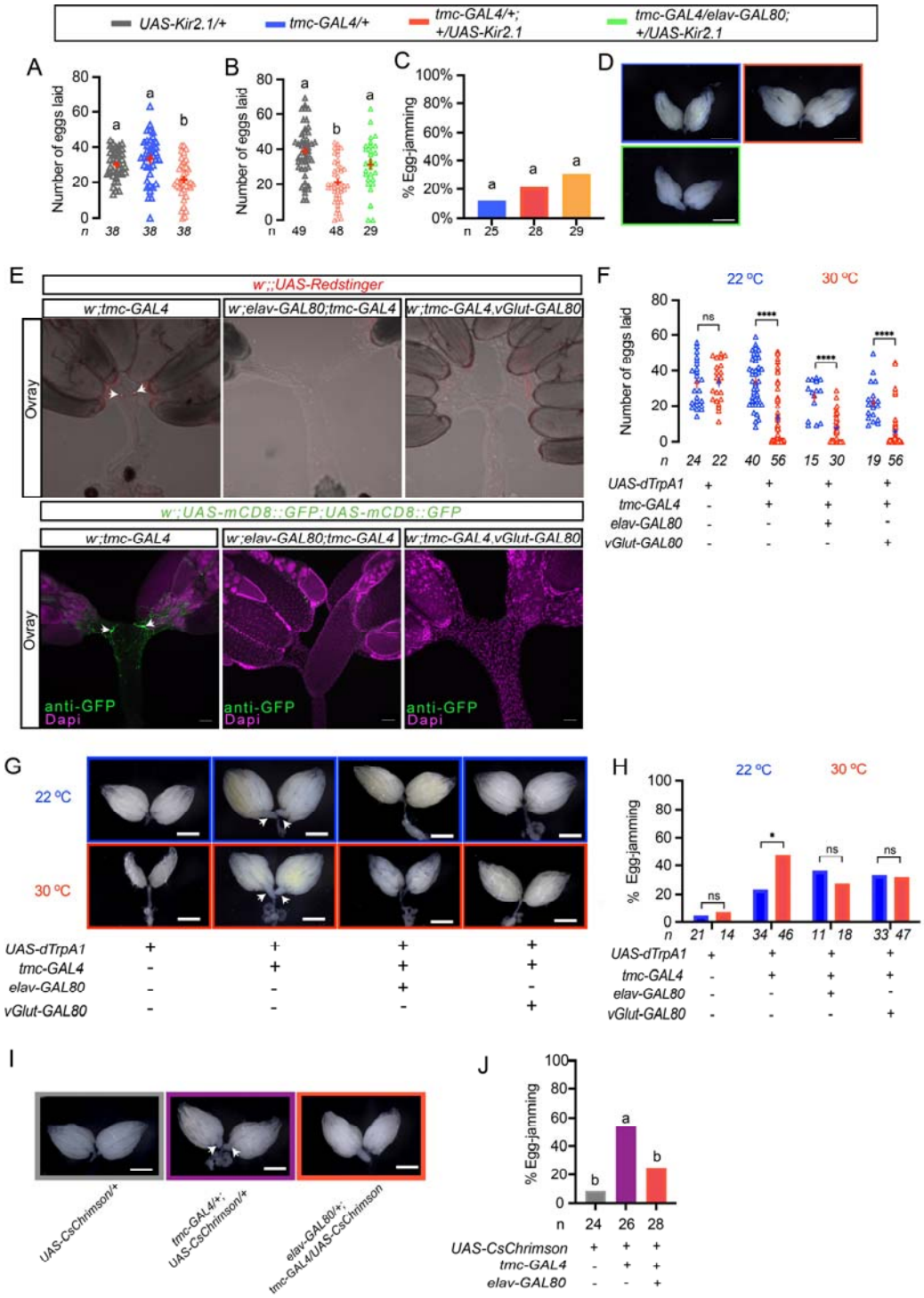

Figure 3. A pair of Tmc-expressing mdn-LO neurons in the lateral oviduct is essential for ovulation, and activation egg-jamming oviduct

In these graphs, *P < 0.05, **P < 0.01, ***P < 0.001, ****P < 0.0001, and ns (non-significant). Groups that share at least one letter are not statistically distinguishable (P > 0.05), whereas groups with completely different letters are

statistically distinguishable ($P < 0.05$).

(**A**) The number of eggs laid per female is reduced when the mdn-LO neurons are selectively silenced by expression of the hyperpolarizing channel *Kir2.1* in the *tmc-GAL4* line. One-way ANOVA with Tukey's Multiple Range Test. In this and the other figures: Groups that share at least one letter are not statistically distinguishable ($P > 0.05$), whereas groups with completely different letters are statistically distinguishable ($P < 0.05$). (**B)** The number of eggs laid per female of mdn-LO neurons selectively silenced, using Kir2.1, in the presence and absence of suppression by *elav-GAL80*. The number of eggs laid is restored by neuron-specific *elav-GAL80* suppression. One-way ANOVA with Tukey's Multiple Range Test. (**C**) The egg-jamming ratio of *UAS-Kir2.1/+, tmc-GAL4/*+, *tmc-GAL4/*+;*UAS-Kir2.1/+,* and *tmc-GAL4/elav-GAL80*;*UAS-Kir2.1/*+ flies. Fisher's exact test. (**D**) Representative images of ovaries of *UAS-Kir2.1/+, tmc-GAL4/*+, *tmc-GAL4/*+;*UAS-Kir2.1/+,* and *tmc-GAL4/elav-GAL80*;*UAS-Kir2.1/*+ flies. (**E**) Using the nuclear-localized RFP (UAS-Redstinger) and the membrane-localized GFP (UAS-mCD8::GFP; UAS-mCD8::GFP) as a marker, we investigated the labeling of mdn-LO neurons in the lateral oviducts in the presence of vGlut-GAL80 and elav-GAL80 strains. Both vGlut-GAL80 and elav-GAL80 can effectively block the tmc-GAL4 labeling of lateral oviduct neurons (mdn-LO) but not neurons in the CNS. Arrowheads indicate the mdn-LO neurons in the lateral oviducts. (**F**) Thermogenetic activation of tmc neurons affects oviposition. The number of eggs laid per female with *UAS-dTrpA1/+, tmc-GAL4/UAS-dTrpA1*, *elav-GAL80;tmc-GAL4/ UAS-dTrpA1*, and *tmc-GAL4,vGlut-GAL80/*+; *UAS-dTrpA1/*+ in 22°C and 30°C. One-way ANOVA with Tukey's Multiple Range Test. (**G**) Representative images of ovaries from *UAS-dTrpA1/+, tmc-GAL4/UAS-dTrpA1, elav-GAL80;tmc-GAL4/ UAS-dTrpA1*, and *tmc-GAL4,vGlut-GAL80/+; UAS-dTrpA1/*+ flies at 22°C and 30°C. (**H**) The egg-jamming ratio of *UAS-dTrpA1/+, tmc-GAL4/UAS-dTrpA1*, *elav-GAL80;tmc-GAL4/ UAS-dTrpA1*, and *tmc-GAL4,vGlut-GAL80/*+; *UAS-dTrpA1/*+ flies. Fisher's exact test

(**I**) Representative images of *UAS-CsChrimsonmVenus*/+ and *tmc-GAL4/*+;*UAS-CsChrimsonmVenus/*+ ovaries after optogenetic activation. The arrow indicates the location where the egg is jamming in the oviduct. (**J**) Optogenetic activation of *tmc-GAL4* neurons using CsChrimson. The egg-jamming ratio after optogenetic activation of *tmc-GAL4* neurons. Fisher's exact test.

Figure 3 —figure supplement 1

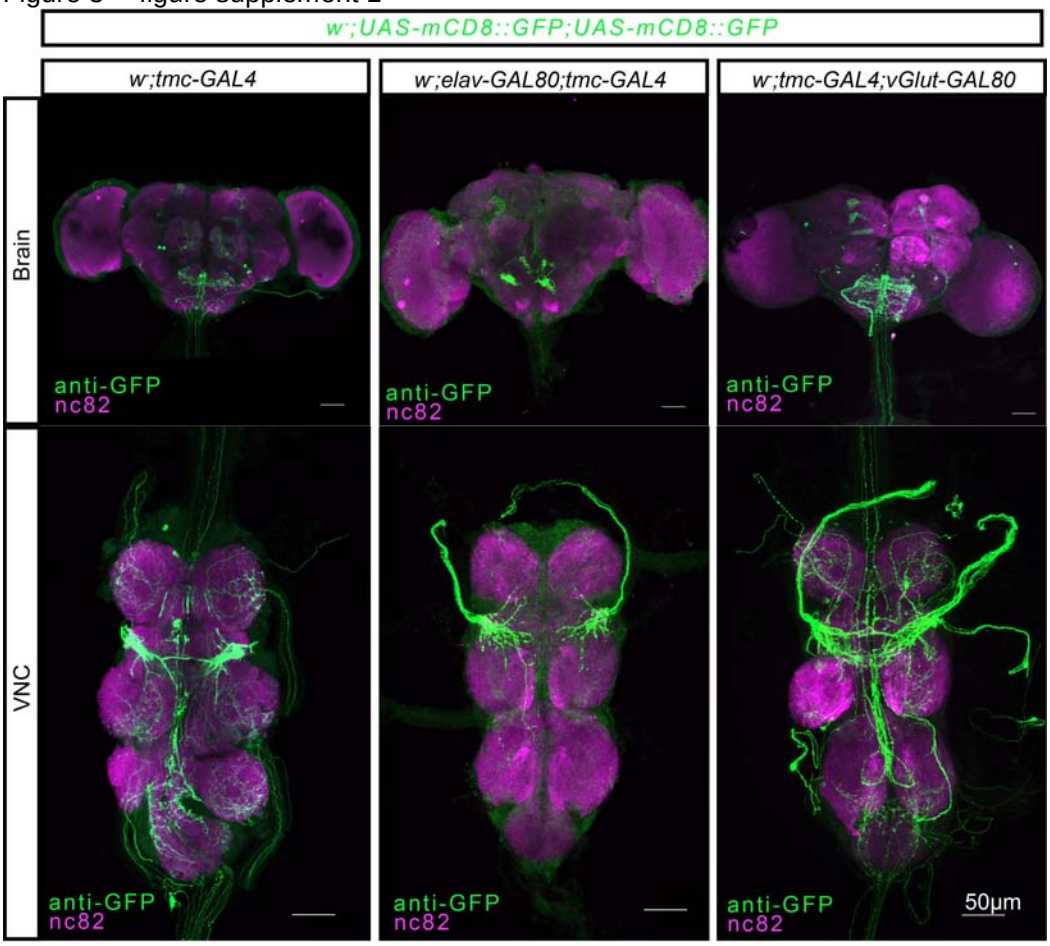

Figure 3—figure supplement 1. Expression of tmc-GAL4 in the presence of different GAL80 in the brain and ventral nerve cord.

Using the membrane-localized GFP (*UAS-mCD8::GFP; UAS-mCD8::GFP*) as a marker, we investigated the labeling of mdn-LO neurons in the CNS in the presence of *vGlut-GAL80* and *elav-GAL80* strains. Note that in the *tmc-GAL4, elav-GAL80 > GFP*, only a subset of the GFP-labeled inputs to the subesophageal zone and the metathoracic ganglion of the VNC are retained; in the *tmc-GAL4; vGlut-GAL80 > GFP*, by contrast, there are fewer labeled axons in the ABG, indicating that inputs from the reproductive system are blocked.

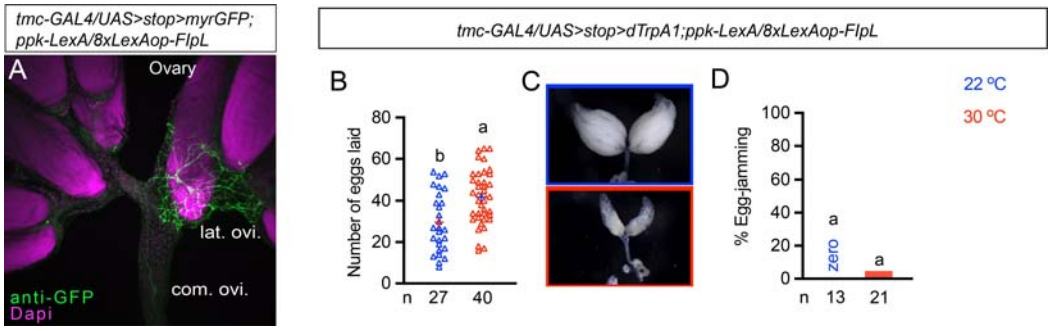

Figure 3—figure supplement 2. Activating mdn-LO neurons on one side only promotes oviposition but does not induce egg-jamming.

In these graphs, groups that share at least one letter are not statistically distinguishable (P >0.05), whereas groups with different letters are statistically distinguishable (P <0.05). (**A**) Using the intersectional technique (*tmc-GAL4/UAS>stop>myrGFP; ppk-LexA/8* × *LexAop-FlpL*) to selectively target mdn-LO neurons revealed the expression of a single mdn-LO neuron in the lateral oviduct on one side only. (**B-C**) Number of eggs laid per female before (22°C) and after thermogenetic (30°C) activation (*TrpA1*) of a single mdn-LO neuron in the lateral oviduct, along with images of the ovaries. Two-tailed t-tests. (**D**) The calculated egg-jamming ratio at 22°C and 30°C of one mdn-LO neuron in the lateral oviduct. Fisher's exact test.

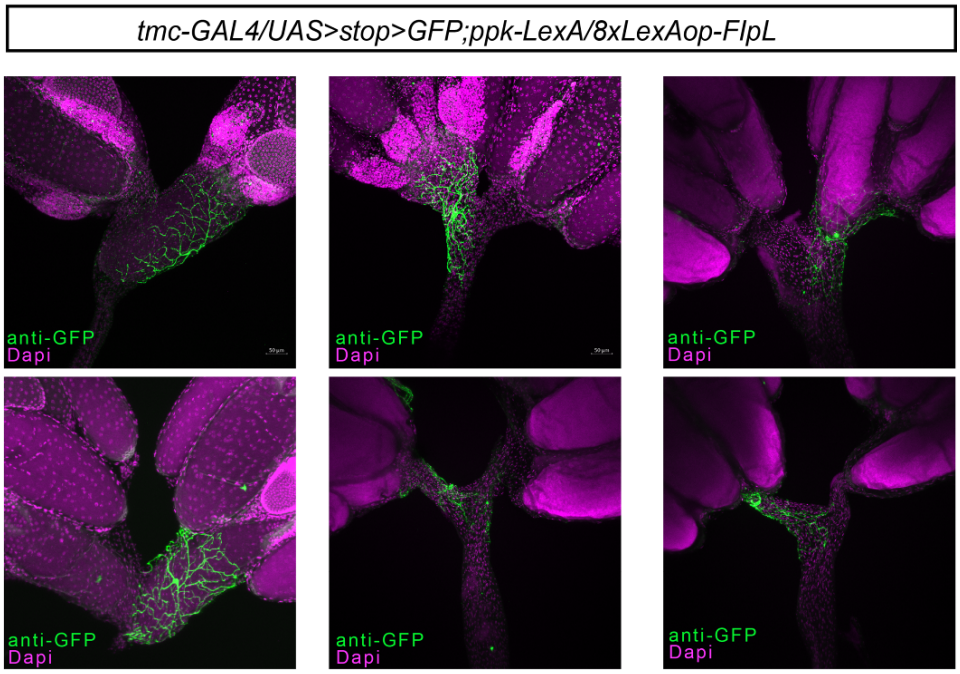

Figure 3—figure supplement 3. Labeling of mdn-LO neuron on one side

Using the intersectional technique (*tmc-GAL4/UAS>stop>myrGFP; ppk-LexA/8* × *LexAop-FlpL*) was used to specifically target mdn-LO neurons. However, in all cases (n=6), it only labeled a single mdn-LO neuron in the lateral oviduct on one side.

tmc-expressing sensory neurons in the reproductive tract can sense contractions of the lateral oviduct tract

Our experiments, so far suggest that the female flies sense the passage of eggs through the reproductive tract by means of mechanosensory neurons. Thus, we next asked whether the mdn-LO neurons monitor oviduct muscle contractions and oviposition.

To investigate whether oviposition and ovulation affect activity in mdn-LO neurons, we conducted an assay using a transcriptional reporter of intracellular Ca^{2+} (TRIC) that monitors sustained neuronal activity [51]. Indeed, we found a significant elevation of TRIC signals, corresponding to increased intracellular Ca^{2+} levels, in mdn-LO neurons of egg-laying virgin flies compared with virgin flies that did not lay eggs,

monitored over 5 days (Figure 4A and A').

Next, to further explore the requirement of mdn-LO neurons for ovulation-induced neuronal activity, we monitored Ca^{2+} dynamics in the cell body of mdn-LO neurons in response to ovulation. To visualize changes in Ca^{2+} levels in cell bodies of mdn-LO, we expressed a transgene encoding the Ca^{2+} sensor GCaMP6m (*UAS-GCaMP6m*) and Tdtomato (*UAS-Tdtomato*) [52] in mdn-LO neurons under the control of the *tmc-GAL4.* We surgically exposed the lateral oviduct region of the female reproductive area, aiming to monitor the fluorescence changes of mdn-LO neurons as the egg passed through the lateral oviduct. However, we found that when the egg passes through the lateral oviduct, an inevitable shift occurs along the Z-axis, causing us to lose the signal. Even with the addition of tdTomato as a negative control, the significant displacement still prevented us from accurately monitoring the true calcium fluorescence signal of mdn-LO under the condition of the egg being squeezed through the oviduct. Therefore, we monitored the activity of mdn-LO neurons when the oviduct undergoes spontaneous contractions. We observed that calcium activity in the cell body of the mdn-LO neuron increased when the muscle contracted (Figure 4B and Movie S1).

We also used another calcium sensor GCaMP7s [53] to monitor activity in axonal termini of mdn-LO neurons in the VNC. This was done since the GCaMP7s signal in *tmc* processes in the VNC is less likely to move out of the focal plane when tract contraction occurs, and thus facilitates measurements. We found that the CGaMP7s signal in the axonal termini of *tmc* neurons increased significantly during oviduct contraction (Figure 4C-C''; Movie S2). To ensure that such GCaMP7 increase was not due to ''local interaction'' between *tmc* and other neurons in the VNC, we physically severed the connection (median abdominal nerve, MAN) between the reproductive tract and the VNC. In these severed preparations, we did not observe a significant GCaMP7s increase in *tmc* axons in the VNC during oviduct contractions (Figure 4D-D''; Movie S3), ruling out the possibility that other neurons locally activate *tmc* axons in the VNC. Thus, our results suggest that the *tmc*-expressing mdn-LO neurons of the oviduct are mechanosensory and can detect contraction/distention of the lateral oviduct.

We next asked whether the mdn-LO neurons receive input from sources other than mechanical stimulation during the ovulation process. The insect neurotransmitter/neuromodulator OA is considered a trigger for ovulation in insects [18], so we tested the effect of OA application on mdn-LO neurons. We found that OA activates calcium in the axon terminations of GCaMP6m expressing mdn-LO neurons both in intact animals and after surgically severing the MAN and thus the connection to the oviduct (Figure 4 —figure supplement 1). This suggests that OA modulates activity in the mdn-LO neurons locally in the VNC.

Finally, we used a chemical-genetic approach [54,55] to stimulate the mdn-LO neurons. We expressed the ATP-gated P2X2 channel, which is not expressed endogenously in flies, and can be used for 'chemogenetic activation' of specific neurons of interest. When stimulating the P2X2 expressing mdn-LO neurons with ATP, a robust contraction of the oviduct muscle was induced (Movie S4). This shows that

mdn-LO mechanosensory neurons in the lateral oviduct can not only sense oviduct contraction but also act through downstream motoneurons to regulate contractions of the lateral oviduct.

Figure 4

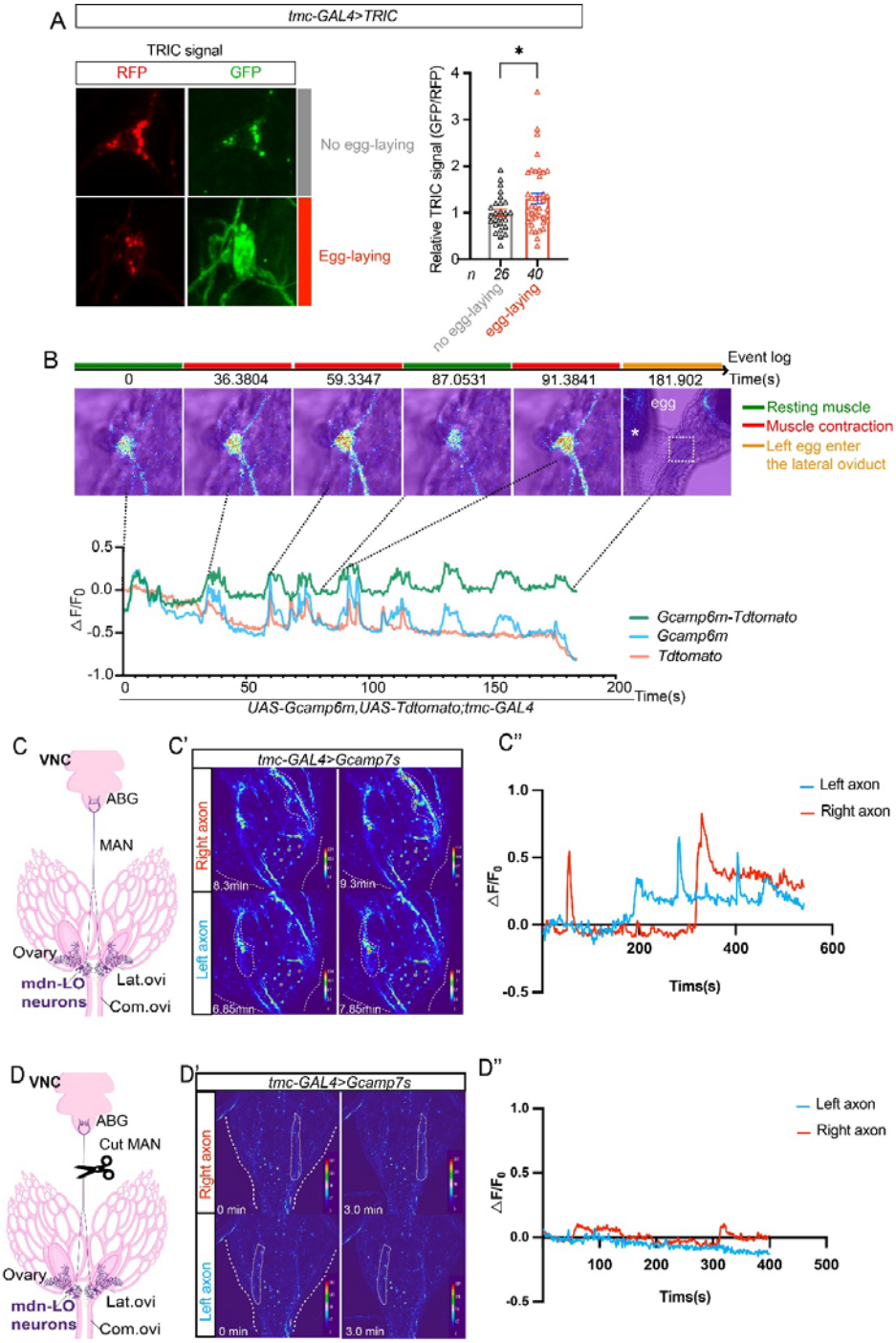

Figure 4. The lateral oviduct *tmc*-expressing neurons (mdn-LO) are mechanosensory and are activated during ovulation.

(**A**) Monitoring sustained calcium activity in mdn-LO neurons using the TRIC method. Comparison of TRIC signals of mdn-LO sensory neurons between egg-laying and non-egg-laying females and representative images. We collected flies that were 5 days post-eclosion and dissected them, separating those that laid eggs and those that did not lay

any eggs. After dissection, without staining, we immediately observed the TRIC signal of mdn-LO in real time under the same parameters (we used GFP/RFP as the TRIC signal). *P < 0.05, **P < 0.01, ***P < 0.001, ****P < 0.0001, and ns (non-significant); Two-tailed t-tests. (**B**) When the lateral oviduct contracts rhythmically, it is accompanied by rhythmic excitation of mdn-LO sensory neurons, as shown by increased Ca^{2+} levels monitored with Gcamp6m. (**C-C''**) In intact animals (median abdominal nerve, MAN, intact), lateral oviduct mdn-LO sensory neurons transmit excitation to the abdominal ganglion (ABG), and Ca^{2+} activity in axon terminations of the left and right neurons can be monitored. (**D- D''**) When the MAN is surgically severed, no Ca^{2+} activity is detected in axon terminations in the ABG during spontaneous muscle contractions. This supports that the activation in intact animals is derived from the axons of the lateral oviduct mdn-LO sensory neurons.

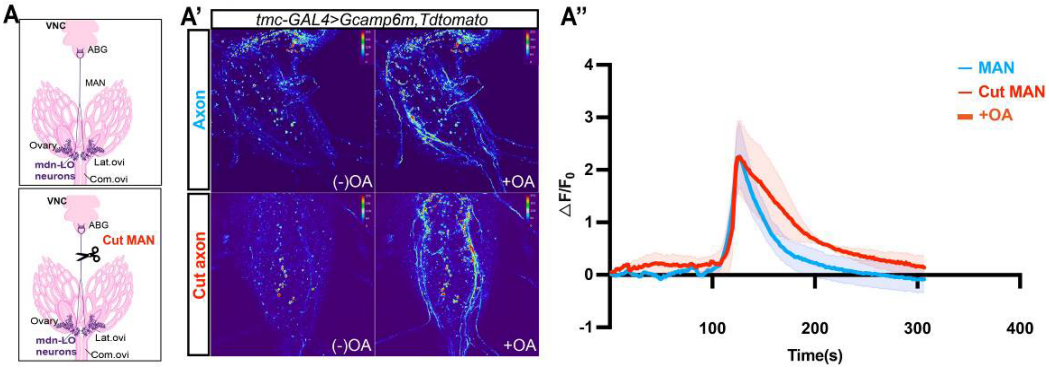

Figure 4—figure supplement 1. Mdn-LO neurons can be activated by octopamine in intact animals and after severing the connection to the reproductive tract.
(A-A'') *tmc*+ neurons can be activated by octopamine (A) Illustration of maintaining the connection via the median abdominal nerve (MAN) and cutting MAN. (A') Calcium imaging of mdn-LO neuron axons in the ABG region before and after the addition of 1 mM octopamine in intact animals and after severing the MAN. (A'') Changes in fluorescence intensity ($\triangle F/F_0$) of Gcamp6m in mdn-LO neuron axons in the ABG region before and after octopamine addition.

ILP7-expressing neurons in the abdominal ganglion receive synaptic input from *tmc*-expressing mdn-LO neurons

We next set out to identify the potential mechanism by which the TMC-expressing mechanosensitive neurons act on neuronal circuits that control oviduct muscle contractions.

First, therefore, we sought to map the postsynaptic targets of mdn-LO neurons by visualization of functionally connected neurons using trans-Tango [56]. We found that expression of trans-Tango in mdn-LO neurons labeled many post-synaptic neurons, primarily in the abdominal ganglion (ABG) (Figure 5A-C'') and suboesophageal ganglion (SEG) (Figure 5—figure supplement 1A). We, however, did not observe that expression of trans-Tango in mdn-LO neurons labeled any post-synaptic local neurons in the ovary or oviduct (Figure 5—figure supplement 1B). This finding

provides further evidence that mdn-LO neurons are sensory neurons that transfer signals to neurons in the central nervous system. Since the trans-Tango labeled numerous neurons, the identification of individual post-synaptic neurons was hard. It has been shown previously [24], and we confirmed here, that some of the *Ilp7-GAL4*-expressing neurons in the ventral portion of the posterior VNC are motor neurons that innervate the oviduct (Figure 5D, Figure 5—figure supplement 2H). Importantly, it was shown that inhibiting ILP7-neurons consistently causes one or more eggs to be jammed in the oviduct [4]. Furthermore, efferent neurons in the VNC that produce OA, identified by a *tdc2-GAL4,* and applied OA, are also involved in the regulation of ovulation [22,57-59]. Thus, we next used the syb:GRASP technique [60] to address the question of whether axons of *tmc*-expressing mdn-LO neurons directly contact processes of *Ilp7*-expressing or *tdc2*-expressing neurons in the abdominal ganglion (ABG). In this method, half of the GFP is targeted specifically to the presynaptic termini of the mdn-LO neurons and the other to *Ilp7* or *Tdc* neurons, and GFP reconstitution occurs at exposure to the synaptic cleft only upon synaptic vesicle fusion. With *Ilp7* neurons and *Tdc* neurons separately as partners, we were able to detect reconstituted GFP clearly in the ABG (Figure 5E-H; Figure 5—figure supplement 2B, D), suggesting that mdn-LO neurons can act as presynaptic partners of both *Ilp7* neurons and *Tdc* neurons in the ABG. However, we did not find evidence with the GRASP technique that *Ilp7* or *tdc2* neurons are coupled pre-synaptically to mdn-LO neurons (Figure 5—figure supplement 1C and 1E). Thus, the activation of mdn-LO neurons by applied OA, shown in Figure 5—figure supplement 1, is likely to represent paracrine (non-synaptic) signaling from octopaminergic neurons. Furthermore, we found that *tdc2*-GAL4 and *Ilp7*-GAL4 signals are not co-expressed in neurons in the ABG or the brain (Figure 5—figure supplement 1I). However, we could show by GRASP that *tdc2* neurons are presynaptically coupled to *Ilp7*-expressing neurons, suggesting functional connections between these neurons (Figure 5—figure supplement 1F-G).

To probe whether the neuronal contacts we observed using the GRASP technique permit the mdn-LO neurons to transmit signals to the *Ilp7*-expressing neurons, we next assessed if we could detect a change in Ca^{2+} levels in the cell bodies and processes of *Ilp7* neurons when we stimulated the mdn-LO neurons. To do this, we developed an *ex vivo* “brain-less” preparation in which the entire ventral nerve cord is dissected together with the full female reproductive tract and intact connections of the nerve supply between the VNC and the reproductive system (but with the connection to the brain is severed). In this *in vitro* preparation, we monitored the Ca^{2+} levels in cell bodies and the processes of *Ilp7*-expressing neurons by using the genetically encoded Ca^{2+} indicator GCaMP6m [52]. To stimulate mdn-LO neurons, we expressed in these neurons the ATP-gated P2X2 channel [54,55].

We found that stimulating the P2X2-expressing mdn-LO neurons with ATP triggered a significant increase in GCaMP signal in the cell bodies of *Ilp7* neurons in the ventral ABG (Figure 5I-O), accompanied by rhythmic contractions of the oviduct (Movie S4). In contrast, exposing control animals that did not express P2X2 in their mdn-LO neurons to the same levels of ATP did not produce an increased GCaMP

signal (Figure 5J). Interestingly, we did not detect an increased GCaMP signal in *Ilp7* neurons located on the dorsal side of the ABG region, only in the ventral cluster, including the female-specific *Ilp7* neurons (Figure 5L). Collectively, our results show that axons of mdn-LO neurons physically contact the *Ilp7* neurons in the ABG, and stimulation of mdn-LO neurons increases Ca^{2+} levels in the cell bodies and processes of ventrally located *Ilp7* neurons (Figure 5M-O).

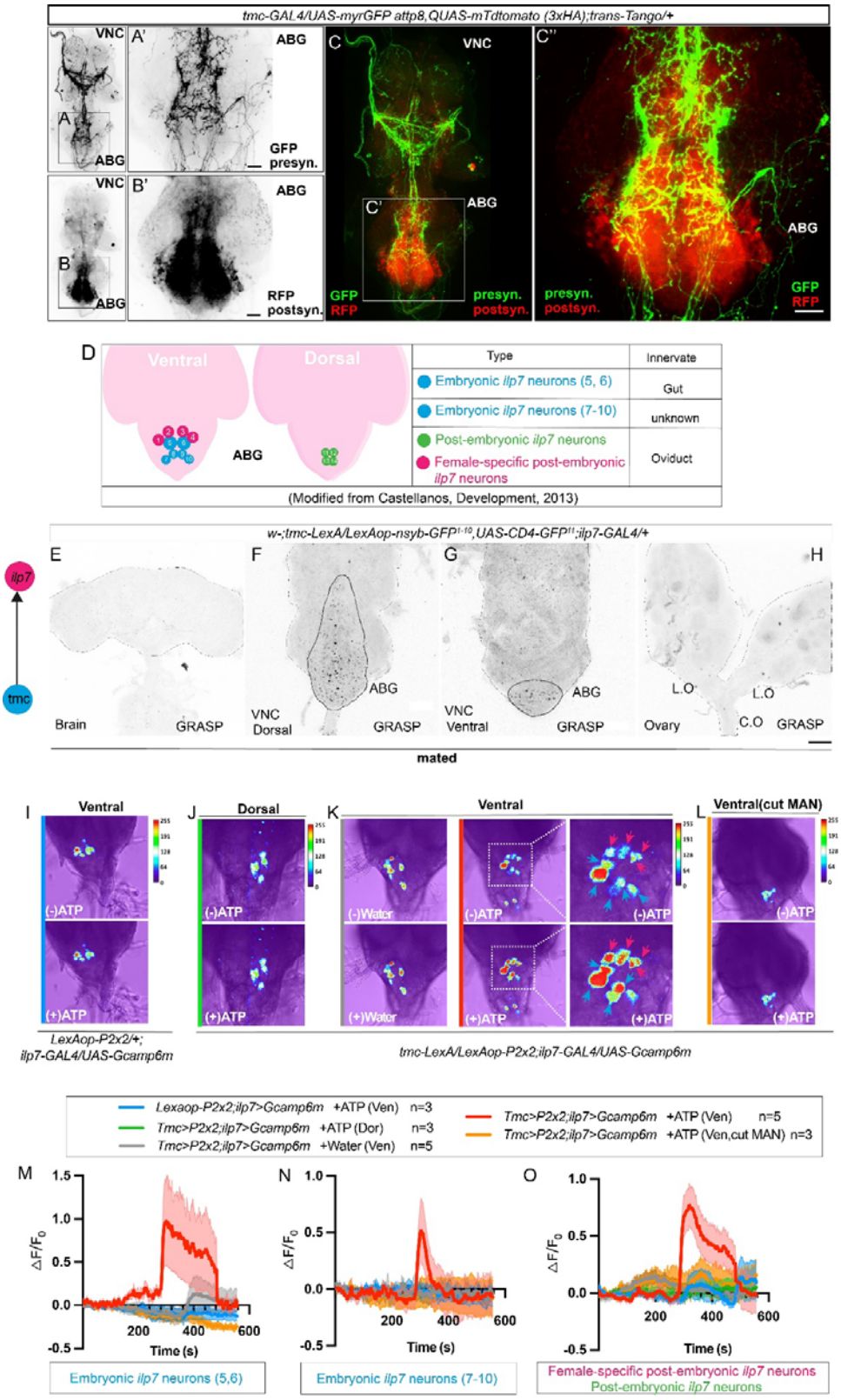

Figure 5. The mdn-LO sensory neurons regulate activity in the *Ilp7* neurons in the ABG, and their connections are visualized by trans-tango and GRASP.

(A-C'') Putative second-order neurons targeted by *tmc*+ neurons (green) in the ABG region

revealed by trans-Tango (red) driven by *tmc*-GAL4. In A-B', we show the expression of presynaptic signal (GFP/dark) in mdn-LO neurons and postsynaptic signal (RFP/dark) of *tmc*+ neurons in the ABG region of VNC. In C-C'' are shown merged confocal images of trans-Tango labeling of postsynaptic neurons (GFP/green) to *tmc*+ neurons (RFP/red).
(D) Location of *Ilp7* neurons in the ventral and dorsal ABG regions. Blue circles indicate embryonic *Ilp7* neurons; pink circles indicate large female-specific post-embryonic *Ilp7* neurons; Green circles indicate the post-embryonic *Ilp7* neurons. Original data from 24. The three types of *Ilp7* -expressing cell clusters innervate different tissues. The embryonic *Ilp7* neurons innervate the intestine, and the female-specific post-embryonic *Ilp7* neurons and post-embryonic *Ilp7* neurons are glutamatergic motoneurons that innervate the oviduct muscle of the female reproductive system. (E-H) GRASP signals between mdn-LO sensory neurons and *Ilp7* neurons observed in the brain, dorsal and ventral VNC, and ovary. (I-L) The mdn-LO sensory neurons regulate the excitation of ventral VNC *Ilp7* neurons in the ABG region. Activating *P2X2*-expressing mdn-LO neurons with 1 mM ATP increased the activity of ventral *Ilp7* motor neurons in the abdominal part of the VNC. The dorsal *Ilp7* neurons are not affected (J). (M-O) Graphs showing activation of *Tmc*+ neurons via *P2X2* increased different *Ilp7*+ motor neuron activity. Fluorescence changes ($\Delta F/F_o$) of *GCaMP6s* in *Ilp7* neurons are shown following different treatments.

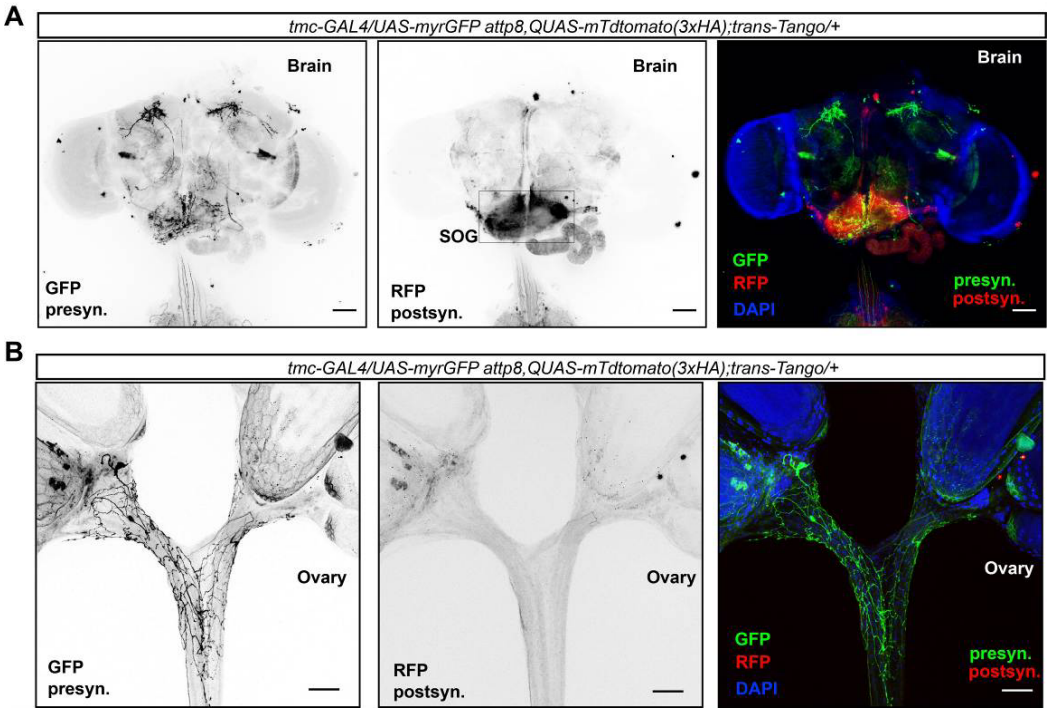

Figure 5—figure supplement 1. The presumed second-order neurons of mdn-LO target the subesophageal ganglion (SEG) region in the brain.
(A) Putative second-order neurons of *tmc*+ neurons (green) in the suboesophageal ganglion (SOG) region revealed by trans-Tango (red). (B) Using the trans-tango system, it was found that there are no putative second-order neurons of mdn-LO in the oviduct.

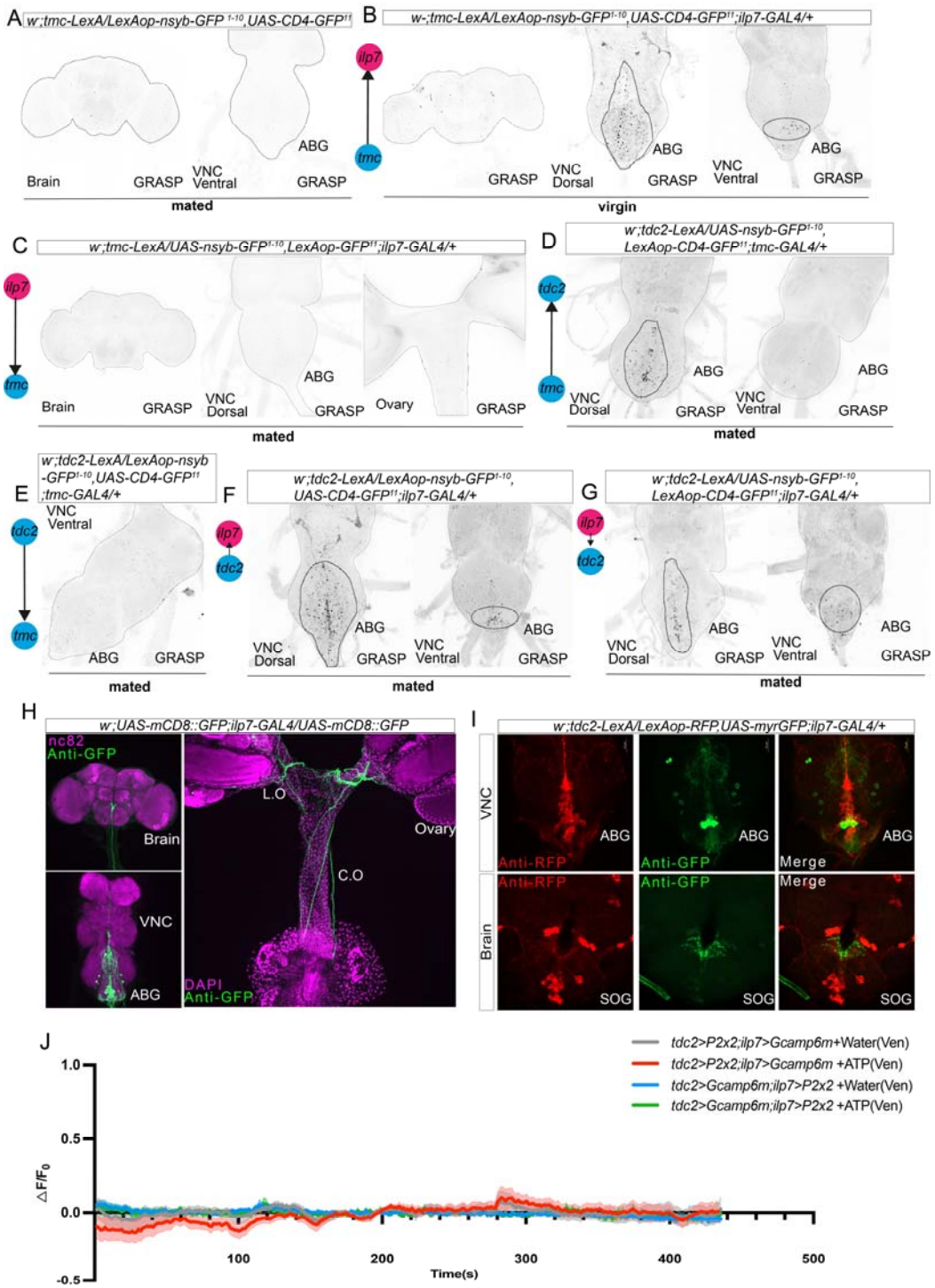

Figure 5—figure supplement 2. Probing connections between *tdc2+*, *Ilp7+*, and *tmc+* neurons by the GRASP technique and calcium imaging.

(A) Lack of GRASP signal from expressing *tmc-LexA* alone in the brain and ventral VNC.

(B) Flies in virgin status were used to obtain the GRASP signal between mdn-LO (expressing *tmc-LexA*) and *Ilp7* + neurons with *Ilp7 -GAL4* in the brain, dorsal, and ventral VNC. The black signal represents the region of putative synaptic connections (indicated by black dashed lines).

(C) No GRASP signal is seen from the *Ilp7* + neurons to *tmc*+ neurons in the brain, dorsal VNC,

and ovary. (D) GRASP signal from the *tmc*+ neurons to *tdc2*+ neurons in the dorsal and ventral VNC. The dark signal represents the region of synaptic connections (indicated by black dashed lines). (E) No GRASP signal is seen from the *tdc2*+ neurons to *tmc*+ neurons in the ventral VNC. (F) GRASP signal from the *tdc2*+ neurons to *Ilp7* + neurons in the ventral and dorsal VNC. The dark signal represents the region of putative synaptic connections (indicated by black dashed lines). (G) GRASP signal from the *Ilp7* + neurons to *tdc2*+ neurons in the ventral and dorsal VNC. The dark signal represents the region of putative synaptic connections (indicated by black dashed lines). (H) The expression of *Ilp7*-GAL4 positive neurons in the brain, VNC, and ovary. (I) *Ilp7*+ (green) and *tdc2*+ (red) neurons within the ABG and brain are distinct. (J) There is no functional connection between ILP7 neurons and Tdc2 neurons. When ILP7 neurons are activated by ATP, the calcium signal in Tdc2 neurons shows no significant change; the converse is also true.

Intrinsic Ca^{2+} oscillations in *Ilp7*-GAL4 neurons are tuned by internal oviduct-linked mechanosensory feedback

We find that in *ex vivo* "brain-free" VNC preparations, *Ilp7*-GAL4–expressing female-specific post-embryonic neurons and embryonic ILP7 neurons display robust rhythmic Ca^{2+} oscillations (Figure 6A, Movie S5-6), with a mean oscillation frequency across all ILP7-neurons of ~0.040 Hz (Figure 6C). To assess whether these oscillations are endogenous or depend on inputs from other VNC neurons, we enzymatically dissociated neurons from surrounding tissue using collagenase and protease while preserving the overall integrity of the preparation. Under these conditions, ILP7-neurons retained slower rhythmic Ca^{2+} oscillations (Figure 6B, Movie S7), with a mean frequency of ~0.019 Hz across cells (Figure 6C), consistent with an intrinsic oscillatory activity. From these experiments we do not have clear evidence that the ILP7-neurons are the *bona fide* pacemaker neurons, but propose that they are integral parts of a CPG circiut.

To search for candidate genes supporting oscillatory conductances in ILP7-neurons, we queried a VNC single-cell transcriptomic resource (Fly Cell Atlas). Within the $nSyb^{+}$ neuronal compartment, an *Ilp7*-positive cluster was delineated by *Ilp7* transcript signal and we subjected this to a screen for enrichment of ion-channel/receptor gene sets (and other genes of interest here). This analysis prioritized genes implicated in Ca^{2+}-coupled membrane oscillations, including I_h (HCN current) [61,62] and Cac (cacophony) [63,64] (Figure 6—figure supplement 1A). These findings provide molecular support for the autonomous rhythmic Ca^{2+} oscillations observed in ILP7-neurons *ex vivo*. Furthermore, we noted expression of vesicular glutamate transporter and the glutamate-gated chloride channel, *GluClα* in ILP7-neurons. We found that glutamate perfusion in the isolated *ex vivo* preparation of VNCs reduced the GCaMP signals in ILP7-neurons (Figure 6—figure supplement 1B-D); possibly related to the enrichment of the GluClα (Figure 6—figure supplement 1A) within the *Ilp7*$^{+}$ cluster.

We next asked whether the rhythmic activity of the ILP7-nerons is modulated by oviduct-linked internal mechanosensory feedback. Specifically, we hypothesized that changes in oviduct geometry during egg transit generate local mechanical forces that,

via mdn-LO mechanosensory afferents innervating the oviduct, modulate the phase and frequency of ILP7-neurons. To test the coupling between oviduct muscle and oscillations in ILP7 neurons, we perturbed the oviduct's configuration in *ex vivo* "brain-free" VNC-oviduct preparations by manually altering the egg's position within the oviduct (see Methods section for details) and monitored the resulting ILP7 activity patterns. We found that manually altering the egg's position in the oviduct affects the Ca^{2+} oscillation patterns of ILP7-neurons (Figure 6D-E). This is likely because different egg positions change the shape of the oviduct, generating mechanical forces sensed by mdn-LO mechanosensory neurons, as demonstrated in previous experiments. Therefore, we propose that internal sensory feedback coordinates insect ovulation by modulating the oscillatory pattern of neurons in the ovulation CPG and thereby affecting oviduct muscle contractions.

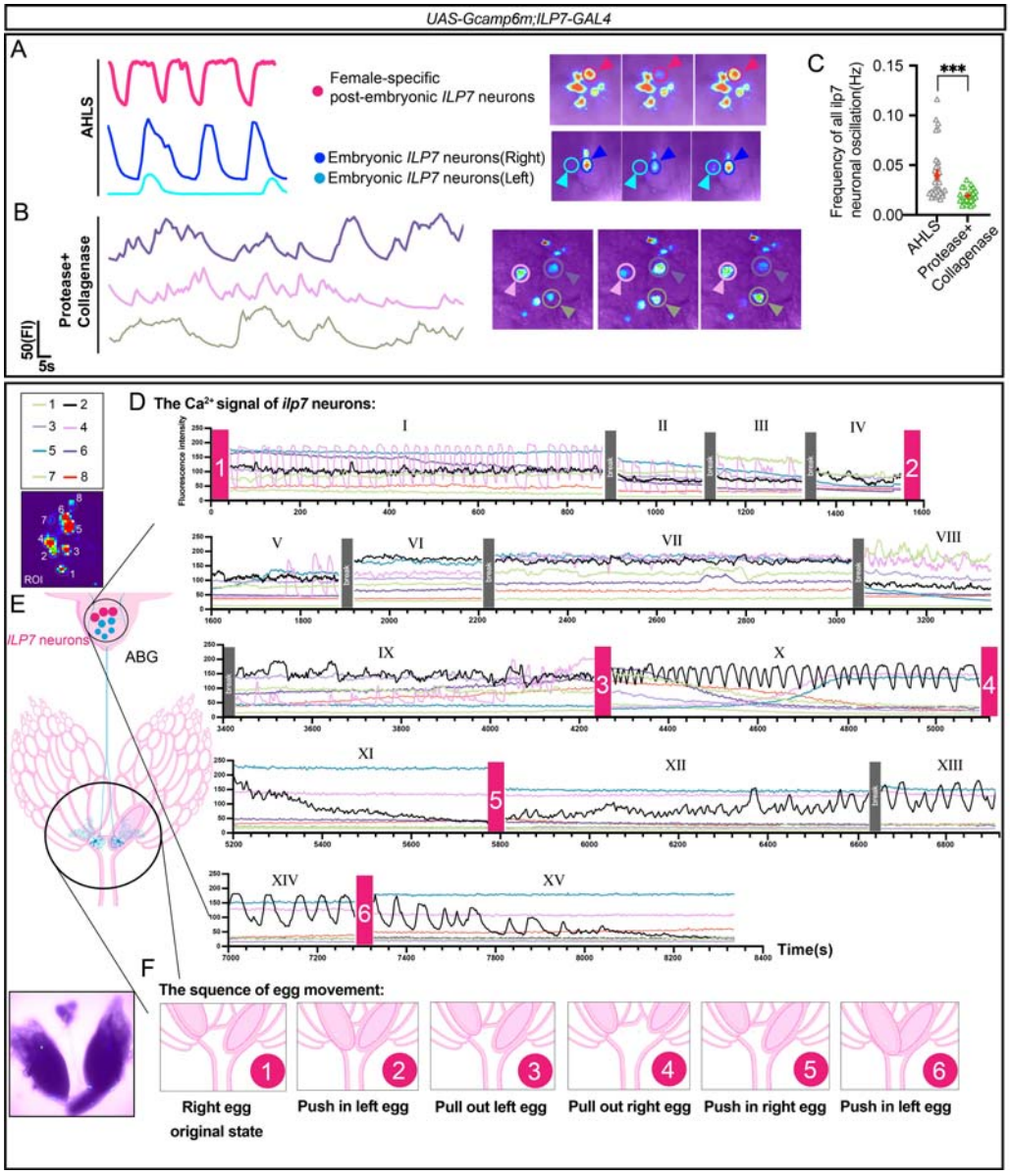

Figure 6. Intrinsic Ca^{2+} oscillations in ILP7-GAL4 neurons are tuned by internal oviduct-linked mechanosensory feedback. (**A**) Intrinsic rhythmic Ca^{2+} oscillations imaged with Gcamp6m in Female-specific post-embryonic ILP7-neurons (pink) and embryonic ILP7-neurons (dark blue and light blue) *in vivo*. (**B**) Intrinsic rhythmic Ca^{2+} oscillations imaged with Gcamp6m in ILP7-neurons after enzymatic digestion *in vivo*. (**C**) The oscillation frequency of ILP7-neurons before and after enzymatic digestion. AHLS(*Drosophila* Adult Hemolymph-Like Saline) (**D**) The Ca^{2+} signal of ILP7-neurons depends on egg locations (moved manually). The numbers in the red squares correspond to the different locations of the egg in panel F. The gray squares represent the recording intervals, during which no egg manipulations were performed. Roman numerals I-XV represent a total of 15 recordings. I-IV shows the signal of ILP7 neurons in the initial state (G1, where the right egg enters the oviduct), where cell 4 exhibits rhythmic calcium oscillations, gradually decreasing in frequency and stopping at 4. V-IX shows the calcium signal after pushing in the left egg (G2). After the left egg is pushed in, cell 4, which had stopped oscillating, suddenly exhibits a short burst of calcium oscillations before stopping, then reappearing at 9. X shows the calcium signal after the left egg is pushed out (G3), with cells 1, 6, and 8 showing a decrease in calcium signal, cell 4 stopping oscillation, and cells 4 and 5 showing an increase in calcium signal. Cell 2 exhibits a calcium oscillation pattern that was not previously present. The signal of cell 2 (XI) decreases after the right egg is pushed out (G4) and increases and re-oscillates after the right egg is pushed back in (G5) (XII-XIV), indicating that the periodic oscillation of cell 2 is regulated by right-side sensory feedback. When the left egg is pushed back into the oviduct, the calcium oscillations of cell 2 disappear (XV). (**E**) An illustration of the pattern during calcium signal recording, with only the ABG region of the VNC retained for detection. The upper part shows the eight ILP7 neurons being monitored and the color of the calcium signals, consistent with Figure E. (**F**) An illustration of the pattern of changing egg positions, with the numbers representing the sequence of events corresponding to Figure D.

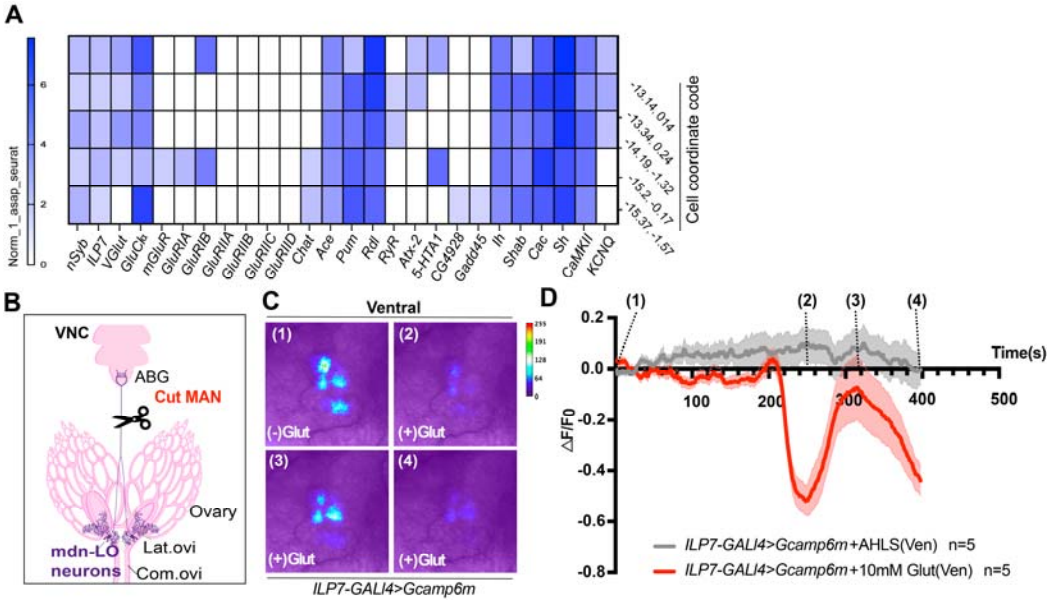

Figure 6—figure supplement 1

(A) Single-cell transcriptomic screen of the adult ventral nerve cord (VNC) (Fly Cell Atlas, Body 10×, stringent set) showing normalized expression of selected ion channels and glutamatergic receptors (and other relevant genes) across cell coordinates provided by Fly Cell Atlas. Within the nSyb□ neuronal compartment, the *Ilp7*□ cluster exhibits enrichment for genes linked to Ca^{2}□ oscillations, including I_h (HCN current) and *Cac* (Cav2 α1 subunit), and for the inhibitory glutamate-gated chloride channel *GluClα*. Note also expression of vesicular glutamate transporter (vGluT) indicative of glutamatergic phenotype of ILP7-neurons. (B) Schematic of the VNC-only *ex vivo* preparation. The abdominal ganglion (ABG) is retained while peripheral reproductive nerves are severed (Cut MAN), isolating central circuits from the ovary/oviduct to permit direct pharmacology on the VNC. (C) Representative images of ventral *Ilp7-GAL4* > *GCaMP6m* somata before and during glutamate perfusion. Panels (1)–(4) correspond to the time points marked in D. (D) Population traces of ILP7 somatic Ca^{2}□ signals ($\Delta F/F_o$, mean ± SEM) under control saline (gray) or 10 mM glutamate (red) perfusion in the VNC-only preparation (n = 5 animals per condition).

Activation of *Ilp7* neurons induces egg-jamming, and ILP7 release affects oviposition

Although previous studies reported that hyperpolarization of *Ilp7-GAL4* neurons in the VNC with *Kir2.1* [65] consistently causes one or more eggs to be jammed in the oviduct due to defects in ovulation coordination [4,8,24], the effects of depolarizing these neurons and ILP7 peptide (Insulin-like peptide 7) on ovulation and oviposition have not been investigated. Therefore, we sought to determine whether depolarization of *Ilp7-GAL4* neurons, induced by mdn-LO sensory neuron activity, results in disrupted ovulation coordination. Additionally, we assessed whether the ILP7 neuropeptide released upon *Ilp7-GAL4* neuron activation plays any role in ovulation and oviposition.

We found that activating the output of *Ilp7*-expressing neurons thermo-genetically by using the *Ilp7-GAL4* to direct the expression of dTrpA1 lead to decreased oviposition and increased egg jamming at 30°C (Fig. 7A-C). Furthermore, optogenetic stimulation of *Ilp7-GAL4*-labeled neurons in *UAS-CsChrimsonvenus/ILP7-GAL4* females induced egg-jamming phenotypes in all individuals (Figure 7D).

When ILP7 levels were reduced by RNAi (*ilp7-GAL4>UAS-Ilp7*-RNAi) during TrpA1 activation of *Ilp7*-neurons, the number of eggs laid was partly restored compared to *Ilp7-GAL4* neuron activation alone (Figure 7A). However, the occurence of egg jamming was not significantly reduced (Figure 7B), similar to the activation of mdn-LO neurons shown in our study. These findings suggest that the ILP7 neuropeptide released during ILP7-neuron activation reduces egg laying, but does not significantly impact the bilateral coordination of ovulation. This might be due to action of the ILP7 peptide on the common oviduct rather than the lateral ones.

Our results indicate that the ovulation-coordinating ILP7 motor neurons are modulated by sensory feedback from the mdn-LO mechanosensory neurons in the lateral oviducts, thereby ensuring the coordination of the ovulation process. These neurons appear to act synaptically (via glutamate) on muscle of the lateral oviducts and via non-synaptic peptidergic action on other muscle.

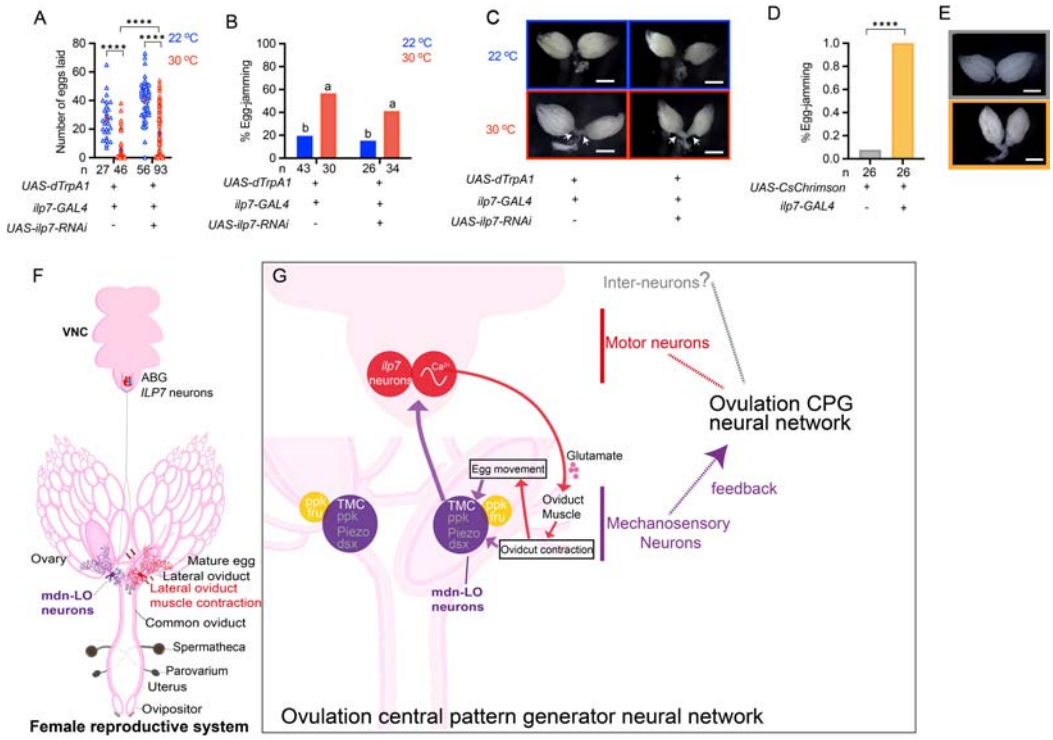

Figure 7. Activation of ILP7 neurons induces egg-jamming, and ILP7 release affects oviposition

Groups that share at least one letter are not statistically distinguishable ($P > 0.05$), whereas groups with completely different letters are statistically distinguishable ($P < 0.05$). * $P < 0.05$, ** $P < 0.01$, *** $P < 0.001$, **** $P < 0.0001$,and ns (non-significant). **(A)** Number of eggs laid per female in flies with ILP7 neurons thermogenetically activated and ILP7 peptide RNAi (*ILP7*-GAL4>UAS-dTrpA1, *ILP7*-GAL4>UAS-dTrpA1/UAS-*ILP7*-RNAi) for 14 h at 22 °C and 30 °C. One-way ANOVA with Tukey's Multiple Range Test. **(B)** The egg-jamming ratio after thermogenetic activation of *Ilp7*-GAL4 neurons and *Ilp7* RNAi. Genotypes as in **A**. Fisher's exact test. (**C**) Representative images of ovaries of *ILP7*-GAL4>UAS-dTrpA1, *ILP7*-GAL4>UAS-dTrpA1/UAS-*ILP7*-RNAi at 22 °C and 30 °C. (**D**) The egg-jamming ratio is increased after optogenetic activation of *ILP7*-GAL4 neurons. (**E**) Representative images of *UAS-CsChrimsonmVenus*/+ and *UAS-CsChrimsonmVenus/ILP7-GAL4* ovaries after optogenetic activation. The arrow indicates the location where the egg is jamming in the oviduct. (**F**) Graphic summary of the female reproductive tract and ventral nerve cord (VNC). (**G**) Graphic summary of the motor neurons and mechanosensory neurons as part of the ovulation central pattern generator circuit. Furthermore (not shown in the figure), *tdc*-expressing (octopaminergic) neurons are found by GRASP to form contacts with ILP7-neurons and applied OA activates mnd-LO neurons (non-synaptically). Importantly, octopamine is involved in triggering and regulating ovulation.

Discussion

Here, we have identified a novel role for the mechanosensory channel protein, TMC, in a pair of multidendritic sensory neurons in the lateral oviducts that provide feedback to a CPG and motor circuits that ensure coordinated ovulation in *Drosophila*. These novel neurons, which we designated mdn-LO, also express two other mechanosensory channels, PPK and PIEZO. Mutations in all three channel proteins result in defects in ovulation and oviposition, whereas mutation or cell-specific knockdown of *tmc* further increases the incidence of egg jamming at the junction between the two lateral and the common oviduct. This indicates that all three mechanosensitive channels are involved in the mechanosensation of the lateral oviduct and that they function complementarily in this sensory process. Thus, the delicate process of ovulation and oviposition requires both “belt and suspenders,”, i. e. several types of multidendritic neurons and mechanosensory channels to ensure efficient proprioceptive feedback to motor circuits in the VNC.

TMC proteins have been identified in a range of invertebrates as well as in mammals, including humans [31,37,66-69]. There are eight TMC proteins in mammals [67,68], two in *Caenorhabditis elegans* [66], three in brown planthoppers [37] , and only one in *Drosophila* [28,31]. The first function of a TMC was described in humans and mice where intact TMC1 and TMC2 activity is necessary for cochlear hair-cell function, and mutations in these genes cause deafness [68,70-72]. The TMC proteins are pore-forming subunits of channels required for mechano-transduction currents in hair cells [73]. In *C. elegans,* the *tmc1* gene encodes a sodium-sensitive cation channel that functions in salt gustation and mediates behavioral avoidance at high NaCl concentrations [66]. Furthermore, TMC-1 expressed in nociceptive neurons of *C. elegans* mediates avoidance of alkalines [74]. Interestingly, TMC proteins also modulate egg-laying in nematodes [75,76]. Another study found that TMC-1 affects *C. elegans* development and sexual behavior in a diet-dependent context [77]. In *Drosophila,* the *tmc* gene has been implicated in proprioception during larval locomotion [31], sensing of food texture [28], and discrimination of the texture of egg-laying site [33]. Finally, in the brown planthopper *Nilaparvata lugens,* the orthologous gene *Nltmc3* was found to be highly expressed in the female reproductive tract, including the oviduct [37]. Knockdown of the *Nltmc3* resulted in impaired ovary development and reduced egg laying. Thus, the present study adds an important role of TMC protein as a mechanosensory channel in mdn-LOs in the lateral oviducts that sense the movement of the eggs and thereby provide feedback to a CPG and motoneurons that control oviduct muscle contractions. This proprioceptive feedback ensures smooth passage of eggs into the common oviduct.

The mdn-LO neurons display rhythmic [Ca^{2+}] oscillations during spontaneous and induced contractions of the oviduct muscle, supporting a mechanosensory role. Our experiments show that the mdn-LOs are presynaptic to a set of female-specific efferent neurons in the abdominal ganglion that produce glutamate and the neuropeptide ILP7, here designated ILP7-neurons. We found that chemo-genetically stimulating activity in the mdn-LOs leads to increased [Ca^{2+}] in the *Ilp7*-neurons and

rhythmic contractions in the oviduct muscle. Previous research has demonstrated that activity in these female-specific ILP7-neurons is required for proper ovulation, likely by using glutamate as a neuromuscular neurotransmitter [4,8,22,24]. However, the function of ILP7 was not shown. Our study demonstrates that blocking ILP7 peptide release during activation of ILP7-neurons affects oviposition in *Drosophila,* but does not affect egg jamming. Thus, this peptide may act further down in the common oviduct to modulate contractions (and oviposition). We could show that activation or inactivation of the ILP7-neurons leads to egg-jamming in the common oviduct, whereas activation of mdn-LO neurons results in egg-jamming in the lateral oviducts. Thus, our findings suggest that the two mdn-LO neurons provide sensory feedback from each of the lateral oviducts to modulate alternating activity in the two pairs of ILP7-neurons in order to generate a smooth passage of eggs into the common oviduct. Our data thus suggest that these ILP7-neurons are part of the ovulation CPG circuit that acts in concert with octopaminergic neurons in the control of ovulation (Fig. 7G), as discussed below.

Apart from the ILP7-neurons and mdn-LO neurons shown here and descending neuronal pathways from the brain [3,16], there are additional neurons in the control of ovulation in *Drosophila*. These are a second pair of multidendritic sensory neurons in the lateral oviducts that express PPK, but not the TMC and PIEZO channels [8], and a small set of octopaminergic efferent neurons (*tdc*-neurons) in the abdominal ganglia that innervate muscle of the reproductive tract [17,18,22]. We did not specifically address the function of this second set of sensory neurons, but did investigate the possible interactions between mdn-LOs, *Ilp7*-neurons, and the *tdc2*-expressing octopaminergic neurons.

Using the GRASP technique to reveal synaptic partners, we could not demonstrate inputs from mdn-LO neurons to *tdc*-expressing neurons or vice versa. However, we found that OA applied to the abdominal ganglion induced [Ca^{2+}] increases in the axon terminations of the mdn-LO neurons. Since GRASP analysis could not visualize any synaptic contacts from *tdc2* neurons onto mdn-LOs, we suggest that OA acts after paracrine release (non-synaptic action) to modulate these sensory cells. By severing the axons of the *tdc2* neurons by cutting the nerve from the abdominal ganglion to the reproductive tract, we could demonstrate that this OA action on mdn-LOs occurs locally in the ganglion. Furthermore, using GRASP, we found that the *tdc2*-neurons are presynaptic to the ILP7-neurons. Thus, the *tdc2*-neurons, which are known triggers of ovulation [17,18,22], may also trigger activity in the ILP7-neurons. In summary, we found no evidence that ILP7- and *tdc2*-neurons signal synaptically to mdn-LO neurons, but *tdc2*-neurons may synapse onto ILP7-neurons and also modulate mdn-LOs by paracrine signaling. Thus, while OA released from *tdc2*-neurons is a main trigger of ovulation [17,18,22] it may also be a signal to activate ILP7-neurons and to modulate the activity of mdn-LOs. Interestingly, the mdn-LOs do not provide mechanosensory feedback to *tdc2*-neurons, only the ILP7-neurons. Furthermore, we do not yet have data to clarify the mechanistic role for the octopaminergic modulation of the mdn-LOs.

While these functional interactions delineate key elements of the ovulation control circuit, the precise wiring logic of the rhythm-generating CPG circuit remains unresolved. With a comprehensive female adult VNC connectome becoming available [78], we can in the future test this working model, using connectome-level predictions focused on ILP7-neurons and their mechanosensory and premotor partners. Our findings indicate that ILP7 neurons may possess an intrinsic oscillatory capacity and can be tuned by oviduct-linked mechanosensory feedback. Until female VNC connectivity data are available we may propose that the ILP7 neurons are located within an ovulation CPG network, tuned by oviduct mechanosensory inputs (e.g., from mdn-LO), and acting on downstream motor neurons and effector muscles This network also includes octopaminergic neurons and possibly further excitatory and inhibitory interneurons.

The specific role of the ILP7 peptide in the ovulation circuit remains to be tested in more detail; we only found a possible role in sustaining oviposition. Previous studies detected no effect on ovulation of *Ilp7*-knockdown in the ILP7-neurons [4,24]. However, overexpression of *Ilp7* in *Ilp7* -neurons, or ubiquitously, led to flies that were more susceptible to laying eggs on a high sucrose medium than a regular medium [4]. It is not clear how ILP7 mediates this effect, but it should be noted that apart from the sex-specific ILP7-neurons there are further ILP7-expressing neurons (in both sexes) in the VNC of flies that may play roles in oviposition-related behavior and its relation to gut function and nutritional state [24,79]. Two of these are ascending interneurons that co-express short neuropeptide F (sNPF) and supply axons to the brain [79,80], where they act on the insulin-producing cells (IPCs) to regulate insulin-signaling when flies ingest high-carbohydrate medium [81,82]. While we only investigated the role of the efferent oviduct-innervating ILP7-neurons (with ILP7 as a putative co-transmitter of glutamate), it may be interesting for the future to determine whether these and ascending ILP7/sNPF neurons are functionally coupled and thereby link nutrition and oviposition.

Materials and methods

Animals

Unless otherwise mentioned, all fly stocks were raised in standard cornmeal–molasses–agar medium maintained at 25 ˚C, 60% humidity, and a 12 hr:12 hr light: dark cycle. We used w^{1118} flies as the wild-type strain.

Key resources table

REAGENT or RESOURCE	Source or reference	Identifiers
Antibodies		
Goat anti-Rabbit Alexa 488	Invitrogen	Cat#A11008; RRID:AB_143
Goat anti-mouse Alexa 488	Invitrogen	Cat#A28175; RRID:AB_2536161
Goat anti-mouse Alexa 555	Invitrogen	Cat# A21428; RRID:AB_2535849
Goat anti-mouse Alexa 647	Invitrogen	Cat# A21235; RRID:AB_2535804
Mouse monoclonal anti-Brp	Developmental Studies Hybridoma Bank	Cat# nc82; RRID:AB_2314
Rabbit polyclonal anti-GFP	Invitrogen	Cat# A11122; RRID:AB_221569
Rabbit polyclonal anti-RFP	Invitrogen	
Mouse polyclonal anti-GFP	Invitrogen	
Chemicals, Peptides, and Recombinant Proteins		
4% PFA	Leagene	Cat# DF0134
Agarose	Invitrogen	Cat# 75510-019
Yeast	Angel	N/A
Propionic acid	MACKLIN	Cat# C14876266
Adenosine 50-triphosphate (ATP)	New England Biolabs	Cat# P0756S
VECTASHIELD® Antifade Mounting Medium	Vector Laboratories	H-1000-10
DAPI	Solarbio	Cat# C0060
Phalloidine	Cytoskeleton, Inc	Cat# PHDN1
PBS	Solarbio	Cat# P1022
ReadyProbes 2.5% Normal Goat Serum	Invitrogen	Cat# R37624
Octopamine	Sigma-Aldrich	Cat# O0250

Trehalose	Biosharp	Cat# BS106B
Glutamate	Sigma- Aldrich	W328512
protease	Sigma- Aldrich	P5147
collagenase	Sigma- Aldrich	C0130
Schneider's Drosophila Medium	BasalMedia	C210908

Experimental Models: Organisms/Strains		
w^{1118}	Bloomington Drosophila Stock Center	3605
tmc^{1}	Zhang et al., 2016	BDSC_66556; RRID:BDSC_66556
tmc^{GAL4}	Guo et al., 2016	Flybase: FBal0321088
UAS-tmc/Cyo; tmc^{1}/TM6B	Zhang et al., 2016	BDSC_66560; RRID:BDSC_66560
w^{-};tmc-GAL4	Zhang et al., 2016	
w^{-};;tmc-GAL4		
tmc^{LexA}	This paper	N/A
tmc-LexA	This paper	N/A
$Piezo^{ko}$	Kim et al., 2012	BDSC_58770; RRID:BDSC_58770
ppk^{ESB}	Laboratory of Wei Zhang, Tsinghua Uni	N/A
ppk^{ko} and $Piezo^{ko}$	Laboratory of Wei Zhang, Tsinghua Uni	N/A
$Piezo^{ko}$; tmc^{1}	Laboratory of Wei Zhang, Tsinghua Uni	N/A
UAS-mCD8::GFP; UAS-mCD8::GFP		
UAS-stinger, UAS-Tdtomato	Laboratory of Yufeng Pan, Southeast Uni	N/A
UAS>Stop>myrGFP; 8xLexAop2-FlpL	Laboratory of Yufeng Pan, Southeast Uni	N/A
fru-LexA	Laboratory of Yufeng Pan, Southeast Uni	N/A
ppk-GAL4	Laboratory of	N/A

	Wei Zhang, Tsinghua Uni	
ppk-LexA	Laboratory of Wei Zhang, Tsinghua Uni	N/A
Piezo-GAL4	Bloomington Drosophila Stock Center	BDSC_59266
UAS-Kir2.1	Bloomington Drosophila Stock Center	Flybase:FBtp0125506
UAS-dTrpA1	Hamada et al., 2008	BDSC:26263
UAS-shibire	Klapoetke et al., 2014	N/A
UAS-CsChrimson	Klapoetke et al., 2014	N/A
vGlut-GAL80/Cyo;TM2/TM6B	Bussell et al., 2014	N/A
elav-GAL80;tmc-GAL4		
tmc-GAL4;ppk-GAL80		
UAS-Redstinger	Laboratory of Yufeng Pan, Southeast Uni	N/A
UAS>Stop>dTrpA1; 8xLexAop2-FlpL	Laboratory of Yufeng Pan, Southeast Uni	N/A
w; 10XUAS-IVS-mCD8::RFP attP18 (13XLexAop2-mCD8::GFP)su(Hw)attP8; P(nSyb-MKII::nlsLexADBDo)attP24/Cyo; M(UAS-p65AD::CaM}ZH-86Fb*	Laboratory of Yufeng Pan, Southeast Uni	N/A
20xUAS-Gcamp7s	Laboratory of Yufeng Pan, Southeast Uni	N/A
w-;UAS-tdtomato,UAS-Gcamp6m/Cyo	Laboratory of Yufeng Pan, Southeast Uni	N/A
UAS-P2X$_2$	Lima and Miesenbo¨ ck, 2005	N/A
LexAop-Gcamp6m		
LexAop-P2X$_2$	Gou et al., 2014	BDSC_76030; RRID:BDSC_76030
tdc2-LexA;44588	Laboratory of Zhefeng Gong,	N/A

	Zhejiang University	
Sp/Cyo;ILP7-GAL4/TM6B	Laboratory of Yufeng Pan, Southeast Uni	N/A
tdc2-LexA;ILP7-GAL4	This paper	N/A
tmc-LexA;ILP7-GAL4	This paper	N/A
LexAOP-nSyb-spGFP$^{1-10}$,UAS-CD4-spGFP^{11}; MKRS/TM6B	Macpherson et al., 2015	BDSC_64315; RRID:BDSC_64315
yw,UAS-myrGFP,QUAS-mtdTomato,attp8;trans-Tango,attp40,tubp-FRT-QS/Cyo	Laboratory of Yufeng Pan, Southeast Uni	N/A
w-;UAS-ppk-RNAi attp40	TsingHua Fly Center	N/A
w-;;UAS-ppk-RNAi attp2	TsingHua Fly Center	N/A
w-;UAS-piezo-RNAi attp40	TsingHua Fly Center	N/A
w-;UAS-tmc-RNAi/cyo; MKRS/TM6B		N/A
Software and Algorithms		
FIJI		https://doi.org/10.1038/nme
Prism 9	GraphPad	RRID:SCR_002798
Photoshop	Adobe	RRID:SCR_014199
Illustrator	Adobe	RRID:SCR_010279
ZEN	Zeiss	N/A
Motic Images Plus3.0	Motic	N/A
Motic Images Devices	Motic	N/A
Primer		
Primer1: GGGCACGTTTTGGCTTTGAT		
Primer2: TGCCTCGCTGTCCTTTGTAG		
Primer3: GAACACCATCGTGGGGAACT		
Primer4: AACAAGCGCAGCTGAACAAG		
Other		
Egg-laying device	Gou et al., 2016	N/A
Anatomical tweezers	Dumont	Cat# 0209-5-PO

Genomic DNA and cDNA amplifications.

Genomic DNA was extracted using a buffer (0.1 M Tris-HCl, pH 9.0, 0.1 M EDTA; 1% SDS). In brief, 30 fruit flies were ground with steel beads in the extraction buffer and incubated at 65°C for 1 hour. The samples were then lysed by adding potassium

acetate to a final concentration of 800 mM and incubated on ice for 2 hours. Precipitation was pelleted by centrifugation at 10,000g for 15 min, and the supernatant was collected. The same volume of ethanol was added to the supernatant at -20℃ for 2h. Precipitation was pelleted by centrifugation at 10,000g for 15 min, and the sediment was collected. The pellet was washed with ice-cold 70% ethanol once, and the pellet was dried before resuspended in DEPC water.

Total RNA Extraction was done using the TRizol reagent (Invitrogen, Carlsbad, CA, USA) according to the manufacturer's instructions. The cDNA template used for cloning was synthesized using the Biotech M-MLV reverse transcription kit and the synthesized cDNA template was stored at -20˚C

Egg-laying assays

Unless otherwise mentioned, all egg laying assays were performed with females in darkness with temperature and humidity controlled at 25˚C and 60%, respectively.

The experimental flies were prepared as previously described (Gou et al., 2016; Yang et al., 2015; Gou et al., 2014). Briefly, 20 to 30 females of the appropriate genotypes and 10 to 15 males of mixed genotypes were gathered into a single food vial that was supplied with wet yeast paste. After 5-7 days, the food in the vial became very chewed up by the larvae, and at this point, the females were well-fed but deprived of egg-laying. Thus, they were ready to lay eggs when placed in our egg-laying apparatus (Yang et al., 2015; Gou et al., 2016). We usually let females lay eggs overnight (~14 hr). Groups to be compared were always run in parallel. Note that regardless of the assays we performed, we always assayed at the level of single animals - each data point on a graph denotes the outcome (number of eggs laid) of a single female.

Assessing ovulation efficiency and egg-jamming ratio

We collected some females for ovary dissection before the egg-laying females were put in the oviposition apparatus, and the remaining females had their ovaries dissected just after the egg-laying experiment in the oviposition apparatus.

We assessed whether there is an ovulation defect by counting mature eggs inside the ovaries of the females before and after the egg-laying assay The ovulation efficiency = (Retained mature eggs before egg-laying - Retained mature eggs after egg-laying) / Retained mature eggs before egg-laying.

Before dissection, we used carbon dioxide for brief anesthesia and severed the connection between the VNC and the brain in the flies. This procedure facilitates dissection and removes the brain's inhibitory effect on ovulation, allowing for autonomous ovulation behavior in the flies, which aids in subsequent dissection and frequency statistics of egg jamming.

The frequency of egg jamming is determined by dissecting female fruit fly ovaries and noting the position of the eggs in the oviduct. We define egg jamming as the presence of two eggs retained in the lateral oviducts. This definition includes the egg-jamming phenotype caused by the inactivation/activation of *ILP7*-expressing neurons, which also leads to an extra egg being retained in the main oviduct.

Ovary development measurement

We dissected and made images of the ovaries of virgin flies on d2AAE and d7AAE, respectively. Using Motic Images Devices and Motic Images Plus 3.0 to capture images of the ovaries. By counting the number of retained mature eggs and using FIJI to calculate the ovary's area and the mature egg's length and width, we could determine whether the oogenesis and ovary development process was aberrant.

dTrpA1 activation and shibire inactivation

Experimental flies were maintained at 22 □C, cold anesthetized, and allowed to recover for at least 30 min at 22 □C. The egg-laying apparatus containing flies was then placed at experimental temperatures (30 □C or 22 □C) for 14 hours to record the egg-laying numbers.

CsChrimson activation

For optogenetic stimulation, test flies were collected within 1-3 d after eclosion and transferred into a vial that was supplied with wet yeast paste containing 0.2 mM all-trans-retinal (116–31–4, Sigma- Aldrich). The vials were covered by aluminum foil to protect them from light for 3–4 days before the ovulation. As previously mentioned, we placed the flies in a transparent oviposition device for egg-laying and stimulated the animals with red light (620 nm, 0.03 mW/mm², Vanch Technology, Shanghai, China). Unless otherwise noted, light stimulation was presented continuously throughout the observation period. Light intensity was measured by placing an optical power meter (PS-310 V2, Gentec, Canada) near the location of the glass slide.

Immunostaining and confocal imaging

We generally dissected the brain, VNC, and ovary of four- to eight-day-old females, except for trans-Tango experiments, in which flies were reared at 20℃ on days 15-20. Dissection was in PBS buffer, and tissues were fixed in 4% PFA solution for ~25 min at room temperature. Samples were then washed four times for 10 minutes each with PAT3 wash buffer (0.5% Triton X-100, 0.5% bovine serum albumin in PBS). The tissues were transferred to a block buffer (ReadyProbes™ 2.5% Normal Goat Serum) and incubated at room temperature for 60 minutes. Primary antibodies were added to the samples and incubated for 4h at room temperature. Samples were then incubated overnight at 4°C. Samples were washed four times for 10 minutes each and then incubated with secondary antibodies at room temperature for 4h. Samples were washed four times, each for 10 minutes. If DAPI staining was required, the samples were incubated at room temperature with DAPI (1:1000, Solarbio, Cat# C0060) for 30 minutes. Finally, samples were mounted using an anti-fade mounting medium (Vector Laboratories).

Titers for primary antibodies were as follows: mouse anti-nc82 (Developmental Studies Hybridoma Bank nc82, 1:1000), mouse anti-GFP (1:1000, A11120, Thermo Fisher Scientific), rabbit anti-GFP (1:1000, A11122, Thermo Fisher Scientific), and rabbit anti-RFP (1:1000, 600-401-379, Rockland), rabbit anti-TMC (1:250). Secondary antibodies were Donkey Alexa 488 anti-rabbit, Donkey Alexa 488 anti-mouse, Donkey

Alexa 555 anti-rabbit, and Donkey Alexa 555 anti-mouse (1:500, R37118, R37114, R37119, R37115, Thermo Fisher Scientific).

Samples were imaged at 10X ,20X, or 40X magnification and 1,024 X 1,024 resolution or more on Zeiss LSM980 confocal microscopes (Jena, Germany) at Nanjing Agricultural University. Images were processed with FIJI or ZEN.

For GRASP, we did not stain the samples with anti-GFP and imaged the fixed and washed samples directly.

For Tdtomato and Stinger, we did not stain the samples with anti-GFP and imaged the fixed and washed samples directly.

For oversized images (such as Fig2J, Fig2S3), we used the Fiji plugin: Stitching-Pixelwise Stitching of Images to process the image stitching.

Antibody generation

We selected the last 24 amino acids of the TMC protein (C-DPRSASPEPTVNIIRIDIENEHEK) as the peptide antigen for peptide synthesis and conjugated it to a KLH carrier for immunization. The synthesized peptide antigen was injected into rabbits to generate antibodies (ABclonal antibodies). Drosophila TMC protein antibodies were obtained by affinity purification of the antiserum, and the specificity of the antibodies was verified via Dot□Blot(DB) testing against the naked peptide before experiments. For immunolabeling, the TMC antibody was diluted at a 1:250 ratio.

TRIC

We collected virgin flies with the genotype w*,10XUAS-IVS-mCD8::RFP attP18, {13XLexAop2-mCD8::GFP}su(Hw)attP8; P{nSyb-MKII::nlsLexADBDo}attP24/tmc-GAL4; M{UAS-p65AD::CaM}ZH-86Fb/+ that were enclosed for 5 days and dissected them, separating those that laid eggs and those that did not lay any eggs (number of eggs = 0). After dissection, without staining, we immediately observed the TRIC signal of mdn-LO neurons in real time under the same parameters. We used GFP/RFP in each cell body as the TRIC signal.

Calcium imaging

For in vitro experiments, VNC and ovaries were dissected in *Drosophila* Adult Hemolymph-Like Saline (AHLS) buffer. The cuticle and connective tissue covering the VNC and ovary were removed using fine forceps. The median abdominal nerve, connecting the abdominal ganglion and the reproductive tract, was either kept intact or carefully severed, depending on the experiment.

Calcium imaging was performed on a Zeiss 980 confocal microscope (Jena, Germany) equipped with 10× or 20× objectives. Briefly, cells were scanned with 488□nm and 555□nm lasers at 512□×□512 pixels (or lower) and an 8□bit dynamic range to acquire baseline GCaMP or tdTomato fluorescence. Regions of interest (ROIs) were selected in FIJI, and fluorescence changes were quantified as $\Delta F/F_0 = (F□□□□–□F_0)/F_0$, where F_0 is the mean fluorescence over 30 frames in mdn□LO neurons expressing GCaMP. For *ilp7* or *tdc2* neurons, F_0 was defined as the average fluorescence over 30

frames before solution application. Depending on the experiment, solutions were applied as follows: 10 µL AHLS buffer,10 µL of 100 mM ATP, and 10 µL of 1 mM octopamine in 90 µL AHLS; and 20 µL of 50 mM glutamate in 80 µL AHLS.

For positioning the egg within the oviduct, we used an ex vivo “brain-less” preparation. Using forceps, we rapidly displaced the egg to different locations along the oviduct and, after each displacement, promptly refocused and began recording one or more bouts (with brief pauses between bouts to restart acquisition). This allowed us to capture how mechanosensory feedback arising from changes in egg position modulates the activity of ILP7 neurons.

Pharmacology

To image intrinsic oscillations of *ilp7* neurons, adult female Drosophila ventral nerve cords (VNCs) were dissected in AHL saline following previously described procedures. To isolate *ilp7* neurons, the dissected adult VNCs were transferred to a digestion solution prepared in standard AHL saline containing 0.4 mg/ml protease and 0.1 mg/ml collagenase and incubated at room temperature for 3 h. Control VNCs were incubated in standard AHL saline for 3 h in parallel. Enzymatic digestion was terminated by washing three times with Schneider’s Drosophila Medium supplemented with 10% FBS prior to calcium imaging.

Single-nucleus RNA-sequencing analyses in *ilp7* neurons.

We queried the Fly Cell Atlas (FCA, https://flycellatlas.org/) and focused on the Body (10×, Stringent) dataset of *Drosophila melanogaster* (ASAP). We performed a three-gene co-expression screen: (1) *nSyb* was used as a neuronal marker to restrict the analysis to VNC neurons; (2) *Ilp7* was used to identify *Ilp7*-positive cells; and (3) each candidate gene from our curated list was queried within that set. Cells co-expressing *nSyb* and *Ilp7* were operationally defined as *Ilp7* neurons. For each candidate gene, we recorded its expression within these Ilp7 neurons and mapped the common co-expression to five FCA cell coordinate codes: (−13.14, 0.14), (−13.34, 0.24), (−14.19, −1.32), (−15.20, −0.17), (−15.37, −1.57). Gene expression levels are reported as Norm_1_asap_seurat values as provided by the FCA portal.

Quantification and statistical analysis

We used the GraphPad Prism6 software package to generate graphs and analyze data statistically. We tested whether the values were normally distributed using D’Agostino–Pearson omnibus and Shapiro–Wilk normality tests before performing statistical analysis. When data were normally distributed, we used parametric tests; when data were not normally distributed, we used non-parametric tests. All tests were two-tailed. All data are presented as mean ± s.e.m. We also consistently labeled the sample numbers directly on graphs.

Sample size

Our results were based on an analysis of behavior at the level of single animals. Sample sizes were determined before experimentation based on both variance and effect sizes. All the data are biological replicates.

Acknowledgments

This research was funded by the the National Natural Science Foundation of China (32022011 & 32472542), the National Key Research and Developmental Program of China (2022YFD1700200) and the Fundamental Research Funds for Central Universities of the Central South University (KJJQ2025014).

References

1. Cury, K.M., and Axel, R. (2023). Flexible neural control of transition points within the egg-laying behavioral sequence in *Drosophila*. Nat. Neurosci. *26*, 1054–1067 10.1038/s41593-023-01332-5.
2. Oliveira-Ferreira, C., Gaspar, M., and Vasconcelos, M.L. (2023). Neuronal substrates of egg-laying behaviour at the abdominal ganglion of *Drosophila melanogaster*. Scientific Reports *13*, 21941. 10.1038/s41598-023-48109-1.
3. Vijayan, V., Wang, F., Wang, K., Chakravorty, A., Adachi, A., Akhlaghpour, H., Dickson, B.J., and Maimon, G. (2023). A rise-to-threshold process for a relative-value decision. Nature *619*, 563–571 10.1038/s41586-023-06271-6.
4. Yang, C.H., Belawat, P., Hafen, E., Jan, L.Y., and Jan, Y.N. (2008). Drosophila egg-laying site selection as a system to study simple decision-making processes. Science *319*, 1679.
5. Deady, L.D., and Sun, J. (2015). A follicle rupture assay reveals an essential role for follicular adrenergic signaling in *Drosophila* ovulation. PLOS Genetics *11*, e1005604. 10.1371/journal.pgen.1005604.
6. Hu, Q., and Wolfner, M.F. (2019). The *Drosophila* Trpm channel mediates calcium influx during egg activation. Proceedings of the National Academy of Sciences *116*, 18994-19000. doi:10.1073/pnas.1906967116.
7. Dickson, B.J. (2008). Wired for Sex: The Neurobiology of *Drosophila* Mating Decisions. Science *322*, 904-909. 10.1126/science.1159276.
8. Gou, B., Liu, Y., Guntur, Ananya R., Stern, U., and Yang, C.-H. (2014). Mechanosensitive neurons on the internal reproductive tract contribute to egg-laying-induced acetic acid attraction in *Drosophila*. Cell Rep. *9*, 522-530. http://dx.doi.org/10.1016/j.celrep.2014.09.033.
9. Greenspan, R.J., and Ferveur, J.-F. (2000). Courtship in *Drosophila*. Annual Review of Genetics *34*, 205-232. doi:10.1146/annurev.genet.34.1.205.
10. Hall, J.C. (1994). The mating of a fly. Science *264*, 1702.
11. Kubli, E. (2003). Sex-peptides: seminal peptides of the *Drosophila* male. Cell. Mol. Life Sci. *60*, 1689-1704. 10.1007/s00018-003-3052.
12. Rezával, C., Pavlou, Hania J., Dornan, Anthony J., Chan, Y.-B., Kravitz, Edward A., and Goodwin, Stephen F. (2012). Neural circuitry underlying *Drosophila* female postmating behavioral responses. Curr. Biol. *22*, 1155-1165. https://doi.org/10.1016/j.cub.2012.04.062.
13. Yamamoto, D., and Koganezawa, M. (2013). Genes and circuits of courtship behaviour in *Drosophila* males. Nat. Rev. Neurosci. *14*, 681. 10.1038/nrn3567.
14. Wang, K., Wang, F., Forknall, N., Yang, T., Patrick, C., Parekh, R., and Dickson, B.J. (2020). Neural circuit mechanisms of sexual receptivity in *Drosophila* females. Nature *589*, 577–581 10.1038/s41586-020-2972-7.
15. Wang, F., Wang, K., Forknall, N., Patrick, C., Yang, T., Parekh, R., Bock, D., and Dickson, B.J. (2020). Neural circuitry linking mating and egg laying in *Drosophila* females. Nature *579*, 101-105. 10.1038/s41586-020-2055-9.
16. Nallasivan, M.P., Singh, D.N.D., Saleh, M.S.R.S., and Soller, M. (2024). Sex-peptide targets distinct higher order processing neurons in the brain to

induce the female post-mating response. eLife *13*, RP98283. 10.7554/elife.98283.1.

17. Middleton, C.A., Nongthomba, U., Parry, K., Sweeney, S.T., Sparrow, J.C., and Elliott, C.J.H. (2006). Neuromuscular organization and aminergic modulation of contractions in the *Drosophila* ovary. BMC Biology *4*, 17. 10.1186/1741-7007-4-17.

18. White, M.A., Chen, D.S., and Wolfner, M.F. (2021). She's got nerve: Roles of octopamine in insect female reproduction. J. Neurogenet. *35*, 132-153. 10.1080/01677063.2020.1868457.

19. Yapici, N., Kim, Y.-J., Ribeiro, C., and Dickson, B.J. (2008). A receptor that mediates the post-mating switch in *Drosophila* reproductive behaviour. Nature *451*, 33-37. http://www.nature.com/nature/journal/v451/n7174/suppinfo/nature06483_S1.html.

20. Wolfner, M.F. (2002). The gifts that keep on giving: physiological functions and evolutionary dynamics of male seminal proteins in *Drosophila*. Heredity *88*, 85-93. 10.1038/sj.hdy.6800017.

21. Lee, H.-G., Seong, C.-S., Kim, Y.-C., Davis, R.L., and Han, K.-A. (2003). Octopamine receptor OAMB is required for ovulation in *Drosophila melanogaster*. Developmental Biology *264*, 179-190. https://doi.org/10.1016/j.ydbio.2003.07.018.

22. Deshpande, S.A., Rohrbach, E.W., Asuncion, J.D., Harrigan, J., Eamani, A., Schlingmann, E.H., Suto, D.J., Lee, P.-T., Schweizer, F.E., Bellen, H.J., and Krantz, D.E. (2022). Regulation of *Drosophila* oviduct muscle contractility by octopamine. iScience *25*, 104697. https://doi.org/10.1016/j.isci.2022.104697.

23. Rodríguez-Valentín, R., López-González, I., Jorquera, R., Labarca, P., Zurita, M., and Reynaud, E. (2006). Oviduct contraction in *Drosophila* is modulated by a neural network that is both, octopaminergic and glutamatergic. Journal of Cellular Physiology *209*, 183-198. https://doi.org/10.1002/jcp.20722.

24. Castellanos, M.C., Tang, J.C.Y., and Allan, D.W. (2013). Female-biased dimorphism underlies a female-specific role for post-embryonic Ilp7 neurons in *Drosophila* fertility. Development *140*, 3915. 10.1242/dev.094714.

25. Thompson, K.J. (1986). Oviposition digging in the grasshopper: II. descending neural control. Journal of Experimental Biology *122*, 413-425. 10.1242/jeb.122.1.413.

26. Vyas, M., Parepally, S.K., and Kamala Jayanthi, P.D. (2022). Is the natural instinct to oviposit in mated female oriental fruit fly, *Bactrocera dorsalis* more of a brain-independent act? Frontiers in Physiology *13*, 800441. 10.3389/fphys.2022.800441.

27. Ayali, A., and Lange, A.B. (2010). Rhythmic behaviour and pattern-generating circuits in the locust: Key concepts and recent updates. Journal of Insect Physiology *56*, 834-843. https://doi.org/10.1016/j.jinsphys.2010.03.015.

28. Zhang, Y.V., Aikin, T.J., Li, Z., and Montell, C. (2016). The basis of food texture sensation in *Drosophila*. Neuron *91*, 863-877.

https://doi.org/10.1016/j.neuron.2016.07.013.

29. Coste, B., Mathur, J., Schmidt, M., Earley, T.J., Ranade, S., Petrus, M.J., Dubin, A.E., and Patapoutian, A. (2010). Piezo1 and Piezo2 are essential components of distinct mechanically activated cation channels. Science *330*, 55-60. doi:10.1126/science.1193270.

30. Coste, B., Xiao, B., Santos, J.S., Syeda, R., Grandl, J., Spencer, K.S., Kim, S.E., Schmidt, M., Mathur, J., Dubin, A.E., et al. (2012). Piezo proteins are pore-forming subunits of mechanically activated channels. Nature *483*, 176-181. http://www.nature.com/nature/journal/v483/n7388/abs/nature10812.html#supplementary-information.

31. Guo, Y., Wang, Y., Zhang, W., Meltzer, S., Zanini, D., Yu, Y., Li, J., Cheng, T., Guo, Z., Wang, Q., et al. (2016). Transmembrane channel-like (tmc) gene regulates *Drosophila* larval locomotion. Proc. Natl. Acad. Sci. U S A. *113*, 7243-7248. 10.1073/pnas.1606537113.

32. Hyunjin, L., Hyun Woo, C., Chen, Z., Zee Yong, P., and Young Joon, K. (2016). A pair of oviduct-born *pickpocket* neurons important for egg-laying in *Drosophila melanogaster*. Mol. Cells *39*, 573-579.

33. Wu, S.F., Ja, Y.L., Zhang, Y.J., and Yang, C.H. (2019). Sweet neurons inhibit texture discrimination by signaling TMC-expressing mechanosensitive neurons in *Drosophila*. eLife *8*, e46165. 10.7554/eLife.46165.

34. Lam, R.M., von Buchholtz, L.J., Falgairolle, M., Osborne, J., Frangos, E., Servin-Vences, M.R., Nagel, M., Nguyen, M.Q., Jayabalan, M., Saade, D., et al. (2023). PIEZO2 and perineal mechanosensation are essential for sexual function. Science *381*, 906-910. doi:10.1126/science.adg0144.

35. Yamanouchi, H.M., Tanaka, R., and Kamikouchi, A. (2023). Piezo-mediated mechanosensation contributes to stabilizing copulation posture and reproductive success in *Drosophila* males. iScience *26*, 106617. https://doi.org/10.1016/j.isci.2023.106617.

36. Qin, J., Yang, T., Li, K., Liu, T., and Zhang, W. (2023). Pharyngeal mechanosensory neurons control food swallow in *Drosophila melanogaster*. eLife, 1-24. 10.7554/elife.88614.1.

37. Jia, Y.L., Zhang, Y.J., Guo, D., Li, C.Y., Ma, J.Y., Gao, C.F., and Wu, S.F. (2020). A mechanosensory receptor TMC regulates ovary development in the brown planthopper *Nilaparvata lugens*. Frontiers in Genetics *11*, 1152. 10.3389/fgene.2020.573603.

38. Häsemeyer, M., Yapici, N., Heberlein, U., and Dickson, B.J. (2009). Sensory neurons in the *Drosophila* genital tract regulate female reproductive behavior. Neuron *61*, 511-518. http://dx.doi.org/10.1016/j.neuron.2009.01.009.

39. Court, R., Namiki, S., Armstrong, J.D., Börner, J., Card, G., Costa, M., Dickinson, M., Duch, C., Korff, W., Mann, R., et al. (2020). A systematic nomenclature for the *Drosophila* ventral nerve cord. Neuron *107*, 1071-1079.e1072. https://doi.org/10.1016/j.neuron.2020.08.005.

40. Kimura, K.-i., Hachiya, T., Koganezawa, M., Tazawa, T., and Yamamoto, D.

(2008). Fruitless and doublesex coordinate to generate male-specific neurons that can initiate courtship. Neuron *59*, 759-769. http://dx.doi.org/10.1016/j.neuron.2008.06.007.

41. Pan, Y., Meissner, G.W., and Baker, B.S. (2012). Joint control of *Drosophila* male courtship behavior by motion cues and activation of male-specific P1 neurons. Proc. Natl. Acad. Sci. U S A. *109*, 10065-10070. doi: 10.1073/pnas.1207107109. .

42. Sweeney, S.T., Broadie, K., Keane, J., Niemann, H., and O'Kane, C.J. (1995). Targeted expression of tetanus toxin light chain in *Drosophila* specifically eliminates synaptic transmission and causes behavioral defects. Neuron *14*, 341-351. https://doi.org/10.1016/0896-6273(95)90290-2.

43. Ma, J., and Ptashne, M. (1987). The carboxy-terminal 30 amino acids of GAL4 are recognized by GAL80. Cell *50*, 137-142. https://doi.org/10.1016/0092-8674(87)90670-2.

44. Lee, T., and Luo, L. (1999). Mosaic analysis with a repressible cell marker for studies of gene function in neuronal morphogenesis. Neuron *22*, 451-461. https://doi.org/10.1016/S0896-6273(00)80701-1.

45. Yang, C.-H., Rumpf, S., Xiang, Y., Gordon, M.D., Song, W., Jan, L.Y., and Jan, Y.-N. (2009). Control of the postmating behavioral switch in *Drosophila* females by internal sensory neurons. Neuron *61*, 519-526. http://dx.doi.org/10.1016/j.neuron.2008.12.021.

46. Hamada, F.N., Rosenzweig, M., Kang, K., Pulver, S.R., Ghezzi, A., Jegla, T.J., and Garrity, P.A. (2008). An internal thermal sensor controlling temperature preference in *Drosophila*. Nature *454*, 217-220. http://www.nature.com/nature/journal/v454/n7201/suppinfo/nature07001_S1.html.

47. Bussell, Jennifer J., Yapici, N., Zhang, Stephen X., Dickson, Barry J., and Vosshall, Leslie B. (2014). Abdominal-B neurons control *Drosophila* virgin female receptivity. Curr. Biol. *24*, 1584-1595. https://doi.org/10.1016/j.cub.2014.06.011.

48. Richard, D., Maria, G., Catherine, C., and Aaron, D. (2008). Visualizing glutamatergic cell bodies and synapses in *Drosophila* larval and adult CNS. Journal of Comparative Neurology *508*, 131-152. doi:10.1002/cne.21670.

49. Klapoetke, N.C., Murata, Y., Kim, S.S., Pulver, S.R., Birdsey-Benson, A., Cho, Y.K., Morimoto, T.K., Chuong, A.S., Carpenter, E.J., Tian, Z., et al. (2014). Independent optical excitation of distinct neural populations. Nat. Meth. *11*, 338-346. 10.1038/nmeth.2836 http://www.nature.com/nmeth/journal/v11/n3/abs/nmeth.2836.html#supplementary-information.

50. Hoopfer, E.D., Jung, Y., Inagaki, H.K., Rubin, G.M., and Anderson, D.J. (2015). P1 interneurons promote a persistent internal state that enhances inter-male aggression in Drosophila. eLife *4*, e11346. 10.7554/eLife.11346.

51. Gao, X.J., Riabinina, O., Li, J., Potter, C.J., Clandinin, T.R., and Luo, L. (2015). A transcriptional reporter of intracellular Ca2+ in *Drosophila*. Nature

Neuroscience *18*, 917-925. 10.1038/nn.4016.

52. Chen, T.-W., Wardill, T.J., Sun, Y., Pulver, S.R., Renninger, S.L., Baohan, A., Schreiter, E.R., Kerr, R.A., Orger, M.B., Jayaraman, V., et al. (2013). Ultrasensitive fluorescent proteins for imaging neuronal activity. Nature *499*, 295-300. 10.1038/nature12354 http://www.nature.com/nature/journal/v499/n7458/abs/nature12354.html#supplementary-information.

53. Dana, H., Sun, Y., Mohar, B., Hulse, B.K., Kerlin, A.M., Hasseman, J.P., Tsegaye, G., Tsang, A., Wong, A., Patel, R., et al. (2019). High-performance calcium sensors for imaging activity in neuronal populations and microcompartments. Nat. Methods *16*, 649-657. 10.1038/s41592-019-0435-6.

54. Lima, S.Q., and Miesenböck, G. (2005). Remote control of behavior through genetically targeted photostimulation of neurons. Cell *121*, 141-152. https://doi.org/10.1016/j.cell.2005.02.004.

55. Yao, Z., Macara, A.M., Lelito, K.R., Minosyan, T.Y., and Shafer, O.T. (2012). Analysis of functional neuronal connectivity in the *Drosophila* brain. J. Neurophysiol. *108*, 684-696. 10.1152/jn.00110.2012.

56. Talay, M., Richman, E.B., Snell, N.J., Hartmann, G.G., Fisher, J.D., Sorkaç, A., Santoyo, J.F., Chou-Freed, C., Nair, N., Johnson, M., et al. (2017). Transsynaptic mapping of second-order taste neurons in flies by trans-Tango. Neuron *96*, 783-795.e784. 10.1016/j.neuron.2017.10.011.

57. Rezával, C., Nojima, T., Neville, Megan C., Lin, Andrew C., and Goodwin, Stephen F. (2014). Sexually dimorphic octopaminergic neurons modulate female postmating behaviors in *Drosophila*. Curr. Biol. *24*, 725-730. http://dx.doi.org/10.1016/j.cub.2013.12.051.

58. Li, Y., Fink, C., El-Kholy, S., and Roeder, T. (2015). The octopamine receptor octß2R is essential for ovulation and fertilization in the fruitfly *Drosophila melanogaster*. Arch. Insect Biochem. Physiol. *88*, 168-178. 10.1002/arch.21211.

59. Lim, J., Sabandal, P.R., Fernandez, A., Sabandal, J.M., Lee, H.-G., Evans, P., and Han, K.-A. (2014). The octopamine receptor Octβ2R regulates ovulation in *Drosophila melanogaster*. PLoS ONE *9*, e104441. 10.1371/journal.pone.0104441.

60. Macpherson, L.J., Zaharieva, E.E., Kearney, P.J., Alpert, M.H., Lin, T.-Y., Turan, Z., Lee, C.-H., and Gallio, M. (2015). Dynamic labelling of neural connections in multiple colours by trans-synaptic fluorescence complementation. Nat. Commun. *6*, 10024. 10.1038/ncomms10024 http://www.nature.com/articles/ncomms10024#supplementary-information.

61. Neymotin, S.A., McDougal, R.A., Bulanova, A.S., Zeki, M., Lakatos, P., Terman, D., Hines, M.L., and Lytton, W.W. (2016). Calcium regulation of HCN channels supports persistent activity in a multiscale model of neocortex. Neuroscience *316*, 344-366. https://doi.org/10.1016/j.neuroscience.2015.12.043.

62. Bean, B.P. (2024). Mechanisms of pacemaking in mammalian neurons. The

Journal of Physiology *n/a*. https://doi.org/10.1113/JP284759.

63. Ryglewski, S., Lance, K., Levine, R.B., and Duch, C. (2012). Cav2 channels mediate low and high voltage-activated calcium currents in Drosophila motoneurons. The Journal of Physiology *590*, 809-825. https://doi.org/10.1113/jphysiol.2011.222836.

64. Saras, A., and Tanouye, M.A. (2016). Mutations of the Calcium Channel Gene cacophony Suppress Seizures in Drosophila. PLOS Genetics *12*, e1005784. 10.1371/journal.pgen.1005784.

65. Baines, R.A., Uhler, J.P., Thompson, A., Sweeney, S.T., and Bate, M. (2001). Altered electrical properties in *Drosophila* neurons developing without synaptic transmission. The Journal of Neuroscience *21*, 1523. 10.1523/JNEUROSCI.21-05-01523.2001.

66. Chatzigeorgiou, M., Bang, S., Hwang, S.W., and Schafer, W.R. (2013). tmc-1 encodes a sodium-sensitive channel required for salt chemosensation in *C. elegans*. Nature *494*, 95-99. 10.1038/nature11845.

67. Keresztes, G., Mutai, H., and Heller, S. (2003). TMC and EVER genes belong to a larger novel family, the TMC gene family encoding transmembrane proteins. BMC Genomics *4*, 24. 10.1186/1471-2164-4-24.

68. Kurima, K., Peters, L.M., Yang, Y., Riazuddin, S., Ahmed, Z.M., Naz, S., Arnaud, D., Drury, S., Mo, J., Makishima, T., et al. (2002). Dominant and recessive deafness caused by mutations of a novel gene, TMC1, required for cochlear hair-cell function. Nat. Genet. *30*, 277-284. 10.1038/ng842.

69. Yue, X., Sheng, Y., Kang, L., and Xiao, R. (2019). Distinct functions of TMC channels: a comparative overview. Cellular and Molecular Life Sciences *76*, 4221-4232. 10.1007/s00018-019-03214-1.

70. Kawashima, Y., Kurima, K., Pan, B., Griffith, A.J., and Holt, J.R. (2015). Transmembrane channel-like (TMC) genes are required for auditory and vestibular mechanosensation. Pflugers Arch. *467*, 85-94. 10.1007/s00424-014-1582-3.

71. Kurima, K., Peters, L.M., Yang, Y., Riazuddin, S., Ahmed, Z.M., Naz, S., Arnaud, D., Drury, S., Mo, J., Makishima, T., et al. (2002). Dominant and recessive deafness caused by mutations of a novel gene, TMC1, required for cochlear hair-cell function. Nature Genetics *30*, 277-284. 10.1038/ng842.

72. Kawashima, Y., Kurima, K., Pan, B., Griffith, A.J., and Holt, J.R. (2015). Transmembrane channel-like (TMC) genes are required for auditory and vestibular mechanosensation. Pflügers Archiv - European Journal of Physiology *467*, 85-94. 10.1007/s00424-014-1582-3.

73. Pan, B., Géléoc, Gwenaelle S., Asai, Y., Horwitz, Geoffrey C., Kurima, K., Ishikawa, K., Kawashima, Y., Griffith, Andrew J., and Holt, Jeffrey R. (2013). TMC1 and TMC2 are components of the mechanotransduction channel in hair cells of the mammalian inner ear. Neuron *79*, 504-515. https://doi.org/10.1016/j.neuron.2013.06.019.

74. Wang, X., Li, G., Liu, J., Liu, J., and Xu, X.Z.S. (2016). TMC-1 mediates alkaline sensation in *C. elegans* through nociceptive neurons. Neuron *91*,

146-154. https://doi.org/10.1016/j.neuron.2016.05.023.

75. Yue, X., Zhao, J., Li, X., Fan, Y., Duan, D., Zhang, X., Zou, W., Sheng, Y., Zhang, T., Yang, Q., et al. (2018). TMC proteins modulate egg laying and membrane excitability through a background leak conductance in *C. elegans*. Neuron *97*, 571-585. https://doi.org/10.1016/j.neuron.2017.12.041.

76. Kaulich, E., Walker, D.S., Tang, Y.Q., and Schafer, W.R. (2021). The *Caenorhabditis elegans* tmc-1 is involved in egg-laying inhibition in response to harsh touch. microPublication biology *2021*. 10.17912/micropub.biology.000439.

77. Zhang, L., Gualberto, D.G., Guo, X., Correa, P., Jee, C., and Garcia, L.R. (2015). TMC-1 attenuates *C. elegans* development and sexual behaviour in a chemically defined food environment. Nat. Commun. *6*, 6345. 10.1038/ncomms7345 https://www.nature.com/articles/ncomms7345#supplementary-information.

78. Stürner, T., Brooks, P., Serratosa Capdevila, L., Morris, B.J., Javier, A., Fang, S., Gkantia, M., Cachero, S., Beckett, I.R., Marin, E.C., et al. (2025). Comparative connectomics of *Drosophila* descending and ascending neurons. Nature *643*, 158-172. 10.1038/s41586-025-08925-z.

79. Miguel-Aliaga, I., Thor, S., and Gould, A.P. (2008). Postmitotic specification of *Drosophila* insulinergic neurons from pioneer neurons. PLOS Biology *6*, e58. 10.1371/journal.pbio.0060058.

80. Nässel, D.R., Enell, L.E., Santos, J.G., Wegener, C., and Johard, H.A.D. (2008). A large population of diverse neurons in the Drosophilacentral nervous system expresses short neuropeptide F, suggesting multiple distributed peptide functions. BMC Neuroscience *9*, 90. 10.1186/1471-2202-9-90.

81. Cognigni, P., Bailey, A.P., and Miguel-Aliaga, I. (2011). Enteric neurons and systemic signals couple nutritional and reproductive status with intestinal homeostasis. Cell Metabolism *13*, 92-104. https://doi.org/10.1016/j.cmet.2010.12.010.

82. Prince, E., Kretzschmar, J., Trautenberg, L.C., Broschk, S., and Brankatschk, M. (2021). DIlp7-producing neurons regulate insulin-producing cells in *Drosophila*. Frontiers in Physiology *12*, 630390. 10.3389/fphys.2021.630390.

Movie legend

Movie S1. The video shows that during lateral oviduct contractions, Ca^{2+} levels in mdn-LO neurons increase in phase with muscle contraction, indicating responsiveness to lateral oviduct activity.

Movie S2. With the median abdominal nerve (MAN) intact, Ca^{2+} in mdn-LO axons within the ABG region of the VNC rises markedly during lateral oviduct contractions.

Movie S3. Following transection of the MAN, Ca^{2+} in mdn-LO axons within the VNC ABG region shows no significant increase during lateral oviduct contractions, indicating that mdn-LO conveys signals to the ABG via the MAN.

Movie S4. ATP stimulation of P2X2-expressing mdn-LO neurons produces a pronounced elevation of Ca^{2+} in *ilp7* neurons within the ABG and triggers strong contractions of the lateral oviduct musculature.

Movie S5. The oscillation of the female-specific post-embryonic ilp7 neurons.

Movie S6. The oscillation of the embryonic ilp7 neurons.

Movie S7. The oscillation of the dissociated ilp7 neurons.